Synthesis and Biological Evaluation of *tert*-Butyl Ester and Ethyl Ester Prodrugs of *L*-γ-Methyleneglutamic Acid Amides for Cancer

Md Imdadul H. Khan,[1,†] Fakhri Mahdi,[1,†] Patrice Penfornis,[1] Nicholas S. Akins,[1,‡] Md Imran Hossain,[1,‡] Seong Jong Kim,[2] Suresh P. Sulochana,[3] Amna T. Adam,[1] Tristan D. Tran,[1] Chalet Tan,[3] Pier Paolo Claudio,[1,4,5] Jason J. Paris,[1] Hoang V. Le[1,*]

[1] Department of BioMolecular Sciences and Research Institute of Pharmaceutical Sciences, School of Pharmacy, University of Mississippi, University MS 38677, U.S.A.
[2] Natural Products Utilization Research Unit, United States Department of Agriculture, Agricultural Research Service, University, MS 38677, U.S.A.
[3] Department of Pharmaceutics and Drug Delivery and Research Institute of Pharmaceutical Sciences, School of Pharmacy, University of Mississippi, University MS 38677, U.S.A.
[4] National Center for Natural Products Research, University of Mississippi, University MS 38677, U.S.A
[5] Cancer Center & Research Institute, Department of Radiation Oncology, University of Mississippi Medical Center, Jackson, MS 39216, U.S.A.
[†] These authors contributed equally to this work.
[‡] These authors contributed equally to this work.
* Corresponding author: hle@olemiss.edu

This paper is dedicated to Professor Richard B. Silverman, an inspiring teacher, advisor, and mentor, on the occasion of receiving the 2021 Tetrahedron Prize for Creativity in Organic Chemistry.

Abstract: In cancer cells, glutaminolysis is the primary source of biosynthetic precursors. Recent efforts to develop amino acid analogues to inhibit glutamine metabolism in cancer have been extensive. Our lab recently discovered many *L*-γ-methyleneglutamic acid amides that were shown to be as efficacious as tamoxifen or olaparib in inhibiting the cell growth of MCF-7, SK-BR-3, and MDA-MB-231 breast cancer cells after 24 or 72 h of treatment. None of these compounds inhibited the cell growth of nonmalignant MCF-10A breast cells. These *L*-γ-methyleneglutamic acid amides hold promise as novel therapeutics for the treatment of multiple subtypes of breast cancer. Herein we report our synthesis and evaluation of two series of *tert*-butyl ester and ethyl ester prodrugs of these *L*-γ-methyleneglutamic acid amides and the cyclic metabolite and its *tert*-butyl esters and ethyl esters on the three breast cancer cell lines MCF-7, SK-BR-3, and MDA-MB-231 and the nonmalignant MCF-10A breast cell line. These esters were found to suppress the growth of the breast cancer cells, but they were less potent compared to their parent *L*-γ-methyleneglutamic acid amides. Pharmacokinetic (PK) studies were carried out on the lead *L*-γ-methyleneglutamic acid amide to establish tissue-specific distribution and other PK parameters. Notably, this lead compound showed moderate exposure to the brain with a half-life of 0.74 h and good tissue distribution, such as in the kidney and liver. Therefore, the *L*-γ-methyleneglutamic acid amides were then tested on glioblastoma cell lines BNC3 and BNC6 and head and neck cancer cell lines HN30 and HN31. They were found to effectively suppress the growth of these cancer cell lines after 24 or 72 h of treatment in a concentration-dependent manner. These results suggest broad applications of the *L*-γ-methyleneglutamic acid amides in anticancer therapy.

Keywords: *L*-γ-Methyleneglutamic acid amides, glutaminolysis, breast cancer, glioblastoma, head and neck cancer

1. Introduction

According to the World Health Organization (WHO), breast cancer is the world's most prevalent cancer.[1] In 2020, 2.3 million women were diagnosed with breast cancer, and 685,000 women died from breast cancer worldwide.[1] Also according to the WHO, glioblastoma, a cancer that occurs in the brain or spinal cord[2] and accounts for more than 60% of all brain tumors in adults, is considered to be the deadliest human cancer.[3–5] Only 25% of patients with glioblastoma survive more than one year, and only 5% of patients with glioblastoma survive more than five years.[6] If untreated, glioblastoma can result in death in less than six months.[7] Also, approximately 4% of people in the United States suffer from head and neck cancer.[8] In cancer cells such as breast cancer, glioblastoma, and head and neck cancer, glutaminolysis is the primary source of biosynthetic precursors, fueling the tricarboxylic acid cycle (TCA cycle) with glutamine-derived α-ketoglutarate. The enhanced production of α-ketoglutarate is critical to cancer cells as it provides carbons for the TCA cycle to produce glutathione, fatty acids, and nucleotides, and contributes nitrogens to produce hexosamines, nucleotides, and many nonessential amino acids.[9,10] Recent efforts to develop amino acid analogues to inhibit glutamine metabolism in cancer have been extensive.

Our lab recently reported an efficient synthetic route to *L*-γ-methyleneglutamine (**1**, **Figure 1A**) and its amide derivatives (**3–10**, **Figure 1A**).[11] Many of these *L*-γ-methyleneglutamic acid amides were as efficacious as tamoxifen or olaparib in inhibiting the cell growth of MCF-7 ($ER^+/PR^+/HER2^-$) and SK-BR-3 ($ER^-/PR^-/HER2^+$) breast cancer cells after 24 or 72 h of treatment (**Figure 2**). Structure-activity relationships showed that *L*-γ-methyleneglutamic acid amides with a secondary amine or branched alkyl amine were less potent in inhibiting the growth than amides with a primary amine or aromatic amine. Amides with an aromatic amine were more potent than those with a primary amine. Within each subset, the amines with a stronger electron-withdrawing group exhibited better potency. In general, N-phenyl amides and *N*-benzyl amides exerted concentration-dependent inhibition of growth by 72 h in the three breast cancer cell lines. Furthermore, *N*-benzyl amides with an electron-withdrawing group at the para position, such as **5** and **6**, were the only compounds that inhibited the growth of triple-negative MDA-MB-231 cells commensurate to olaparib. Additionally, these *L*-γ-methyleneglutamic acid amides were also assessed for cytotoxicity to determine whether cytotoxicity contributed to the reduction in cell growth. The results showed that these compounds exhibited selective cytotoxicity and produced necrosis in all three breast cancer cell lines (**Figure 3**). Notably, these *L*-γ-methyleneglutamic acid amides did not inhibit the growth of the nonmalignant MCF-10A breast cells nor produced cytotoxicity in these control cells.[11] MCF-10A has been shown to be a reliable model for nonmalignant human mammary epithelial cells.[12] While their mechanisms of cancer cell cytotoxicity are not known, some of these compounds may involve multiple targets. For instance, compounds **8** and **9** exerted similar potency for MCF-7 cytotoxicity at 24 h, but **9** was much more potent by 72 h, supporting the recruitment of additional receptor interactions, signaling factors, and/or compounding "bystander" cytotoxicity associated with the death of a large proportion of cells.

A) ***L*-γ-methyleneglutamine, *L*-γ-methyleneglutamic acid, and *L*-γ-methyleneglutamic acid amides:**

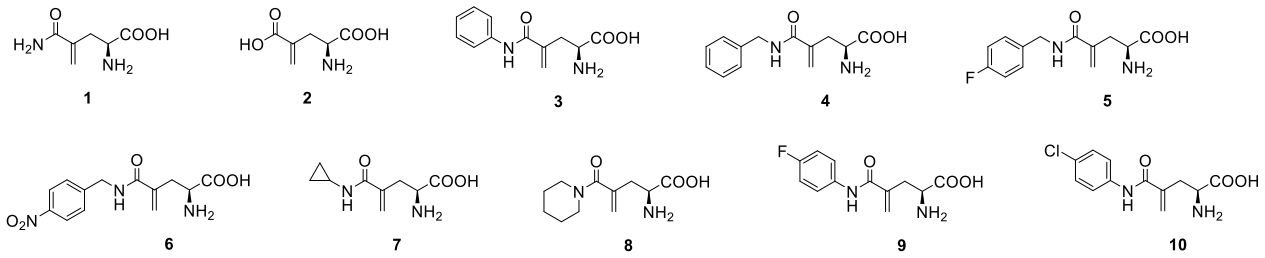

B) ***tert*-Butyl esters of *L*-γ-methyleneglutamic acid amides:**

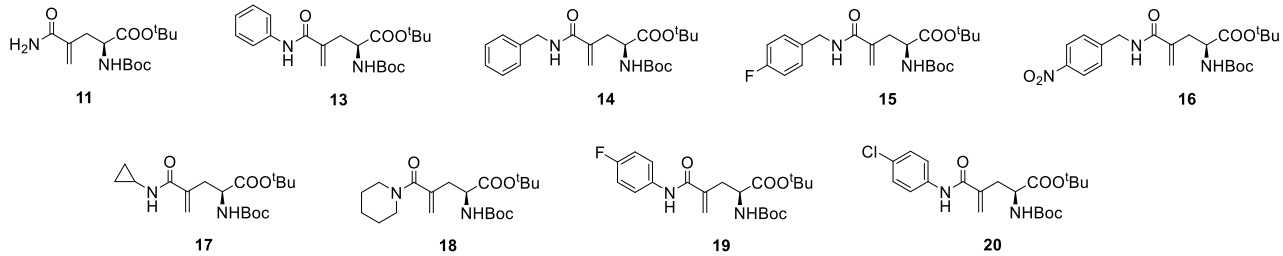

C) **Ethyl esters of *L*-γ-methyleneglutamic acid amides:**

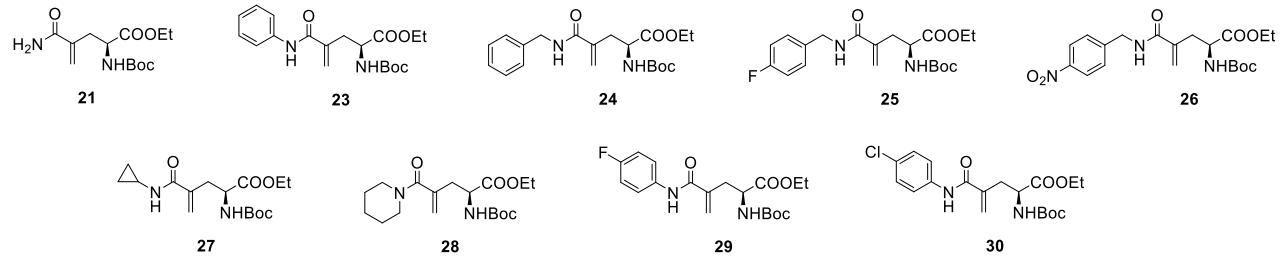

D) **The cyclic metabolite and its *tert*-butyl and ethyl esters:**

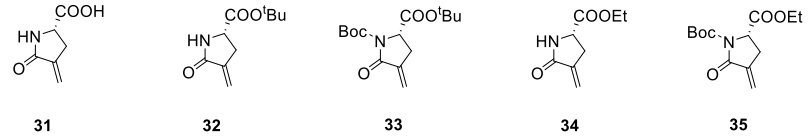

Figure 1. A) Structures *L*-γ-methyleneglutamine (**1**), *L*-γ-methyleneglutamic acid (**2**), and *L*-γ-methyleneglutamic acid amides **3–10**; **B)** Structures of *tert*-butyl esters of *L*-γ-methyleneglutamic acid amides; **C)** Structures of ethyl esters of *L*-γ-methyleneglutamic acid amides; **D)** Structures of the cyclic metabolite and its *tert*-butyl esters and ethyl esters. The numberings 12 and 22 are intentionally skipped so that the structures and numberings are in correspondence among the panels.

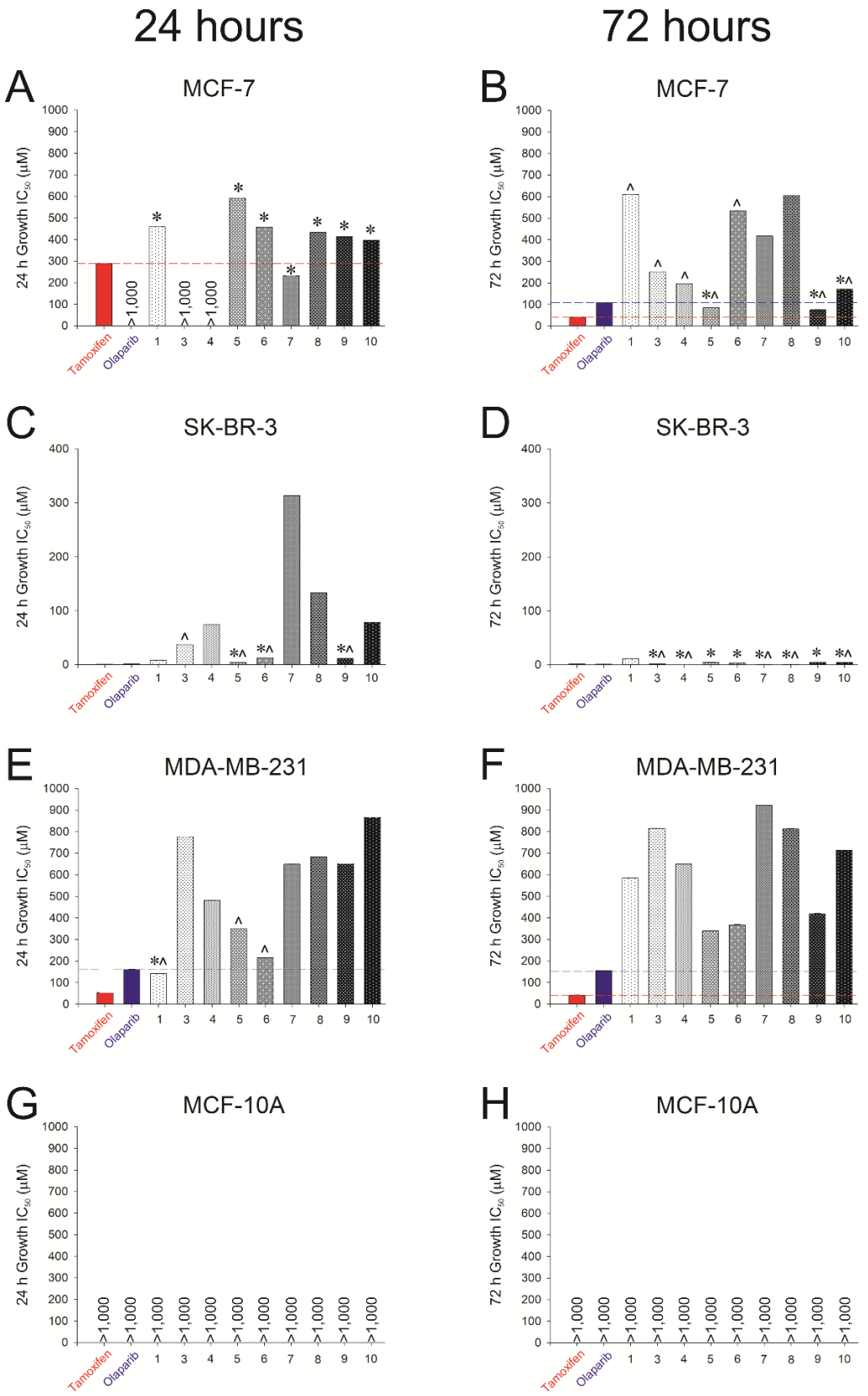

Figure 2. Inhibition of growth of MCF-7, SK-BR-3, and MDA-MB-231 breast cancer cells and nonmalignant MCF-10A breast cells by *L*-γ-methyleneglutamine (**1**) and *L*-γ-methyleneglutamic acid amides **3**–**10** after 24 h and 72 h of treatment. *indicates equipotency to tamoxifen. ^indicates equipotency to olaparib. This figure was created with data from our previous report, which were shown in a table as logIC_{50} values.[11] We used these data to create this figure to make the comparison between the *L*-γ-methyleneglutamic acid amides and the newly synthesized esters easier to visualize.

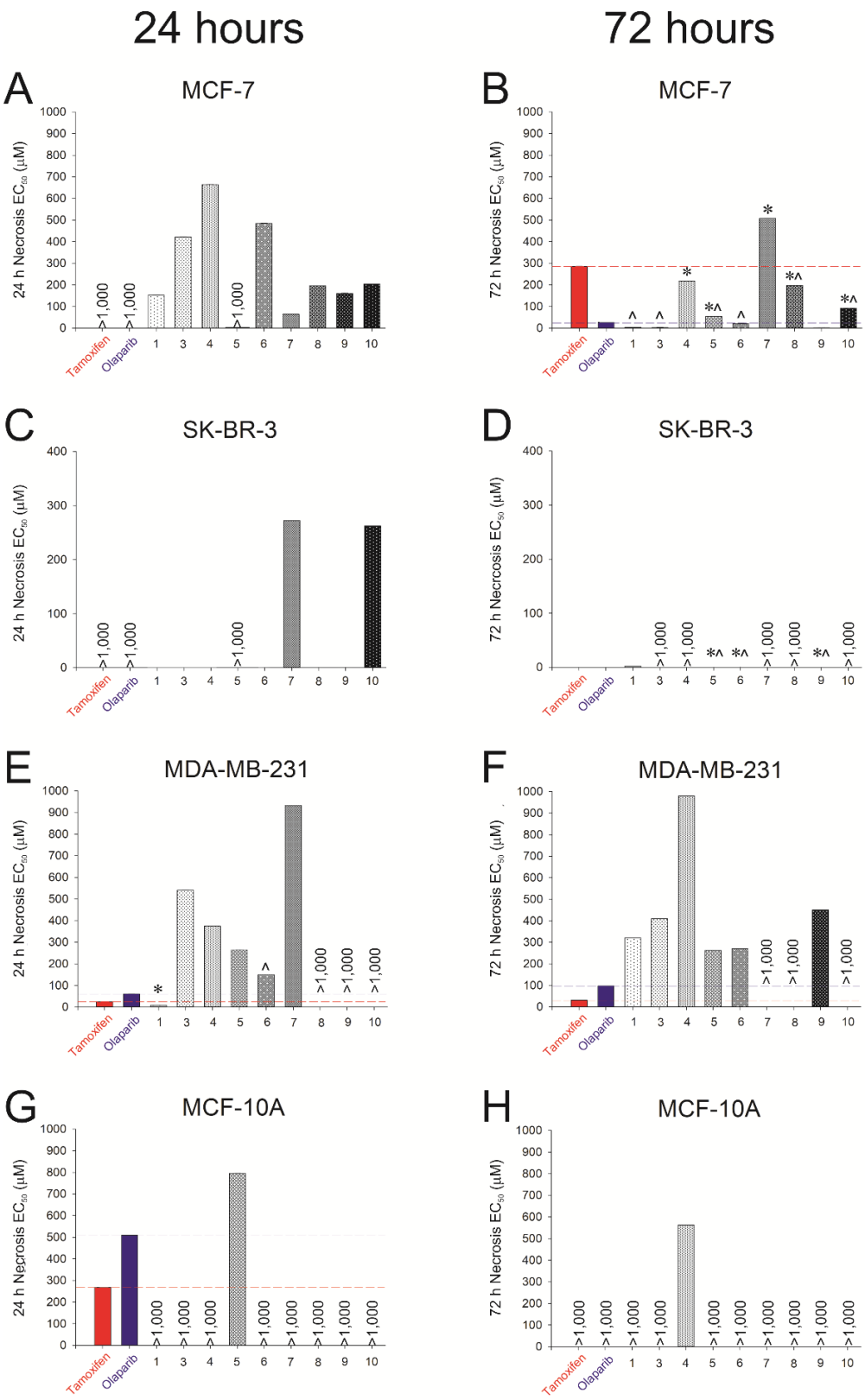

Figure 3. Necrosis of MCF-7, SK-BR-3, and MDA-MB-231 breast cancer cells and nonmalignant MCF-10A breast cells by *L*-γ-methyleneglutamine (**1**) and *L*-γ-methyleneglutamic acid amides **3–10** after 24 h and 72 h of treatment. *indicates equipotency to tamoxifen. ^indicates equipotency to oalparib. #indicates greater potency than either tamoxifen or olaparib. This figure was created with the data from our previous report, which were shown in a table as logEC_{50} values.[11] We used these data to create this figure to make the comparison between the *L*-γ-methyleneglutamic acid amides and the newly synthesized esters easier to visualize.

While the molecular target(s) of these *L*-γ-methyleneglutamic acid amides for the inhibition of cancer cell growth are not known, they did not seem to inhibit the activity of glutamine-dependent enzymes, such as glutaminase.[11] This is good news because glutamine-based glutaminase inhibitors, such as azaserine, acivicin, and DON, produced gastrointestinal toxicity, myelosuppression, and neurotoxicity, due to their non-selective activity on glutamine-dependent enzymes. We speculated that glutamine transporters could be a possible target for these *L*-γ-methyleneglutamic acid amides.[11] They would likely act as reversible inhibitors of glutamine transporters, rather than irreversible inhibitors, due to the low reactive nature of the α,β-unsaturated amide group and the fact that they did not inhibit the activity of glutaminase with pre-incubation nor inhibit the growth or produce cytotoxicity on the nonmalignant MCF-10A breast cells. Glutaminolysis is much more important for cancer cells than for normal cells since normal cells use glycolysis as the primary source of energy and biosynthetic precursors. This would explain why the *L*-γ-methyleneglutamic acid amides did not inhibit the growth or produce cytotoxicity in the nonmalignant MCF-10A breast cells.

As part of our ongoing effort to modify these glutamine-based compounds to develop more selective and efficacious anticancer agents, we synthesized two series of *tert*-butyl ester and ethyl ester prodrugs of the *L*-γ-methyleneglutamic acid amides and the cyclic metabolite and its *tert*-butyl esters and ethyl esters (**Figures 1B–D**) and evaluated them on the three breast cancer cell lines MCF-7, SK-BR-3, and MDA-MB-231. The nonmalignant MCF-10A breast cell line was used as a control. Recognizing that the ester group on these compounds might affect their binding to glutamine transporters, we decided to keep the *N*-Boc group in these ester series to see if we could enhance the availability of these compounds via membrane permeability, instead of glutamine transporters. Two series of free amines and free carboxylic acids of these compounds are being synthesized and studied in our lab. The results have shown that the newly synthesized esters also suppressed the growth of the breast cancer cells, but they were less potent compared to their parent *L*-γ-methyleneglutamic acid amides. Therefore, we performed pharmacokinetic (PK) studies on the lead *L*-γ-methyleneglutamic acid amide (**5**) and determined its C_{max}, T_{max}, mean elimination half-life, mean clearance, and volume of distribution. Notably, **5** showed moderate exposure to the brain with a half-life of 0.74 h and good tissue distribution, such as in the kidney and liver. Therefore, we tested many of these *L*-γ-methyleneglutamic acid amides (**3–9**) on glioblastoma cell lines BNC3 and BNC6 and head and neck cancer cell lines HN30 and HN31. They were found to effectively suppress the growth of these cancer cell lines after 24 or 72 h of treatment. These results suggested broad applications of the *L*-γ-methyleneglutamic acid amides in anticancer therapy.

2. Results and Discussion

2.1. Syntheses of *tert*-butyl esters of the *L*-γ-methyleneglutamic acid amides

The syntheses of *tert*-butyl ester prodrugs of the *L*-γ-methyleneglutamic acid amides (**11** and **13–20**, **Figure 1B**), starting from the commercially available *L*-pyroglutamic acid **41** (**Scheme 1**), were performed by following our previously published report.[11] An esterification of **41** with *tert*-butyl acetate in the presence of perchloric acid[13] produced **42** in 70% yield. A Boc-protecting reaction of the amide[11,14] of **42** gave **43** in 87% yield. Introduction of the methylene group at C4 via a modified α-methylenation method[11,15] produced **33** in 75% yield. The cyclic amide ring in **33** was selectively opened with LiOH[16] to afford **44** in 67% yield (the *tert*-butyl ester remained intact). Finally, an amide coupling reaction[17] of **44** with ammonium chloride or various amines produced the *tert*-butyl esters **11** and **13–20** of the corresponding *L*-γ-methyleneglutamic acid amides in 40–75% yields.

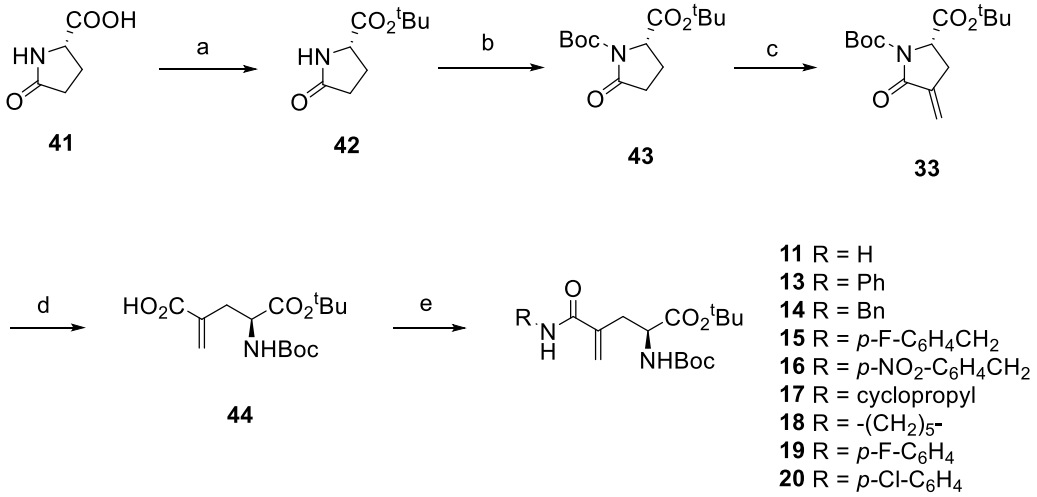

Scheme 1. Syntheses of *tert*-butyl esters of the *L*-γ-methyleneglutamic acid amides (**11–20**). Reagents and conditions: a) AcO^tBu, $HClO_4$, rt, 18h, 70%; b) $(Boc)_2O$, DMAP, Et_3N, CH_2Cl_2, rt, 18 h, 87%; c) i. LiHMDS, $CF_3CO_2CH_2CF_3$, THF, -78 °C, 4 h, ii. $(CHO)_n$, K_2CO_3, 18-crown-6, benzene, reflux, 4 h, 75%; d) LiOH, THF, 23 °C, 18 h, 67%; e) R-NH_2/NH_4Cl, HBTU, Et_3N, *N*-methylmorpholin, THF, 23 °C, 40–75%. Abbreviations: AcO^tBu, *tert*-butyl acetate; $HClO_4$, perchloric acid; $(Boc)_2O$, di-*tert*-butyl dicarbonate; DMAP, 4-dimethylaminopyridine; Et_3N, triethylamine; CH_2Cl_2, methylene chloride; LiHMDS, lithium bis(trimethylsilyl)amide; $CF_3CO_2CH_2CF_3$, 2,2,2-trifluoroethyl trifluoroacetate; THF, tetrahydrofuran; $(CHO)_n$, paraformaldehyde; K_2CO_3, potassium carbonate; LiOH, lithium hydroxide; HBTU, 3-[bis(dimethylamino)methyliumyl]-3*H*-benzotriazol-1-oxide hexafluorophosphate.

2.2. Syntheses of ethyl esters of the *L*-γ-methyleneglutamic acid amides

The syntheses of ethyl ester prodrugs of the *L*-γ-methyleneglutamic acid amides (**21** and **23–30**, **Figure 1C**) started from the commercially available *L*-pyroglutamic acid **41** (**Scheme 2**). Esterification of **41** with ethanol in the presence of sulfuric acid[18] produced **45** in 60% yield. A Boc-protecting reaction of the amide[11,14,19–21] of **45** gave **46** in 91% yield. Introduction of the methylene group at C4 of compound **46** using a modified α-methylenation method[11,15] produced **35** in 55% yield. The cyclic amide ring in **35** was selectively opened with LiOH[16] to afford **47** in 55% yield (the ethyl ester remained intact). Finally, an amide coupling reaction[17] of **47** with ammonium chloride or various amines produced the ethyl esters **21** and **23–30** of the corresponding *L*-γ-methyleneglutamic acid amides in 40–75% yields.

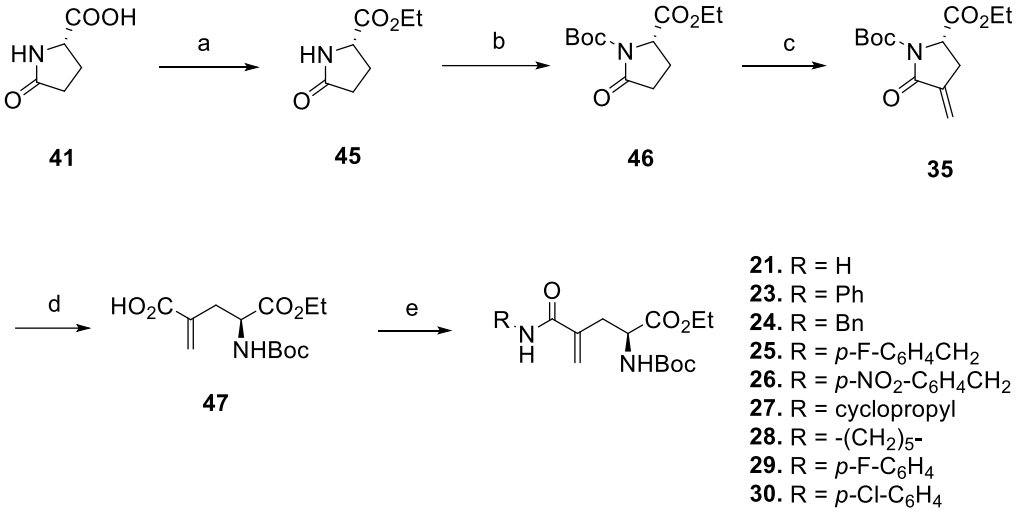

Scheme 2. Syntheses of ethyl esters of the *L*-γ-methyleneglutamic acid amides (**21–30**). Reagents and conditions: a) H_2SO_4, EtOH, rt, 24 h, 60%; b) $(Boc)_2O$, DMAP, Et_3N, CH_2Cl_2, rt, 18 h, 91%; c) i. LiHMDS, $CF_3CO_2CH_2CF_3$, THF, -78 °C, 4 h, ii. $(CHO)_n$, K_2CO_3, 18-crown-6, benzene, reflux, 4 h, 55%; d) LiOH, THF, 23 °C, 18 h, 55%; e) R-NH_2/NH_4Cl, HBTU, Et_3N, *N*-methylmorpholin, THF, 23 °C, 40–75%. Abbreviations: H_2SO_4, sulfuric acid; EtOH, ethanol; $(Boc)_2O$, di-*tert*-butyl dicarbonate; DMAP, 4-dimethylaminopyridine; Et_3N, triethylamine; CH_2Cl_2, methylene chloride; LiHMDS, lithium bis(trimethylsilyl)amide; $CF_3CO_2CH_2CF_3$, 2,2,2-trifluoroethyl trifluoroacetate; THF, tetrahydrofuran; $(CHO)_n$, paraformaldehyde; K_2CO_3, potassium carbonate; LiOH, lithium hydroxide; HBTU, 3-[bis(dimethylamino)methyliumyl]-3*H*-benzotriazol-1-oxide hexafluorophosphate.

2.3. Syntheses of the cyclic metabolite and its *tert*-butyl esters and ethyl esters

In our previous studies, the cyclic **31** (**Figure 1D**) was suggested to be a metabolite of the *L*-γ-methyleneglutamic acid amides **3–10**.[11] This was later confirmed through our PK studies (see Section 2.6). We were wondering if **31** was the metabolite responsible for the anticancer activity of these compounds. Therefore, we synthesized **31**, as well as its *tert*-butyl esters (**32–33**, **Figure 1D**) and ethyl esters (**34–35**, **Figure 1D**) and evaluated them for their anticancer activity. The syntheses of compounds **33** and **35** are shown in **Scheme 1** and **Scheme 2**, respectively. Compounds **31** and **32** were synthesized from **33** while compound **34** was synthesized from **35** (**Scheme 3**). Treatment of **33** with TFA and anisole removed both the *tert*-butyl and Boc protecting groups,[22] providing the desired **31** in 98% yield. Treatment of **33** with 3M HCl removed only the Boc protecting group,[23] affording the desired **32** in 85% yield. Treatment of **35** with 3M HCl[23] produced the desired **34** in 66% yield.

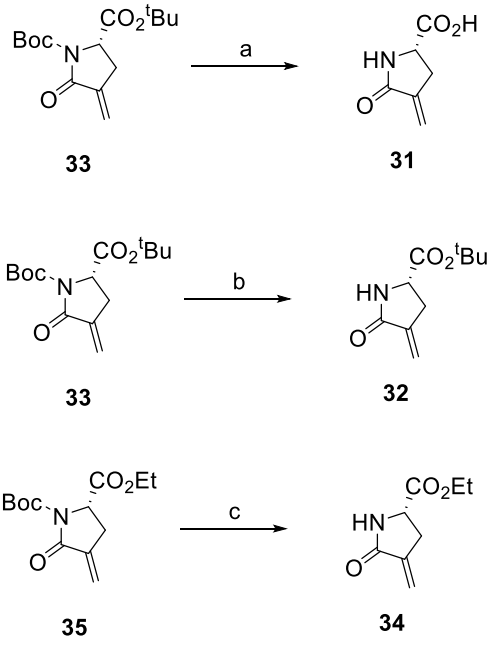

Scheme 3. Syntheses of the cyclic metabolite (**31**) and its *tert*-butyl and ethyl esters. Reagents and conditions: a) TFA, anisole, DCM, rt, 98%; b) 3M HCl, ACN, rt, 85%; c) 3M HCl, ACN, rt, 66%. Abbreviations: TFA, trifluoroacetic acid; DCM, methylene chloride; HCl, hydrochloric acid; ACN, acetonitrile.

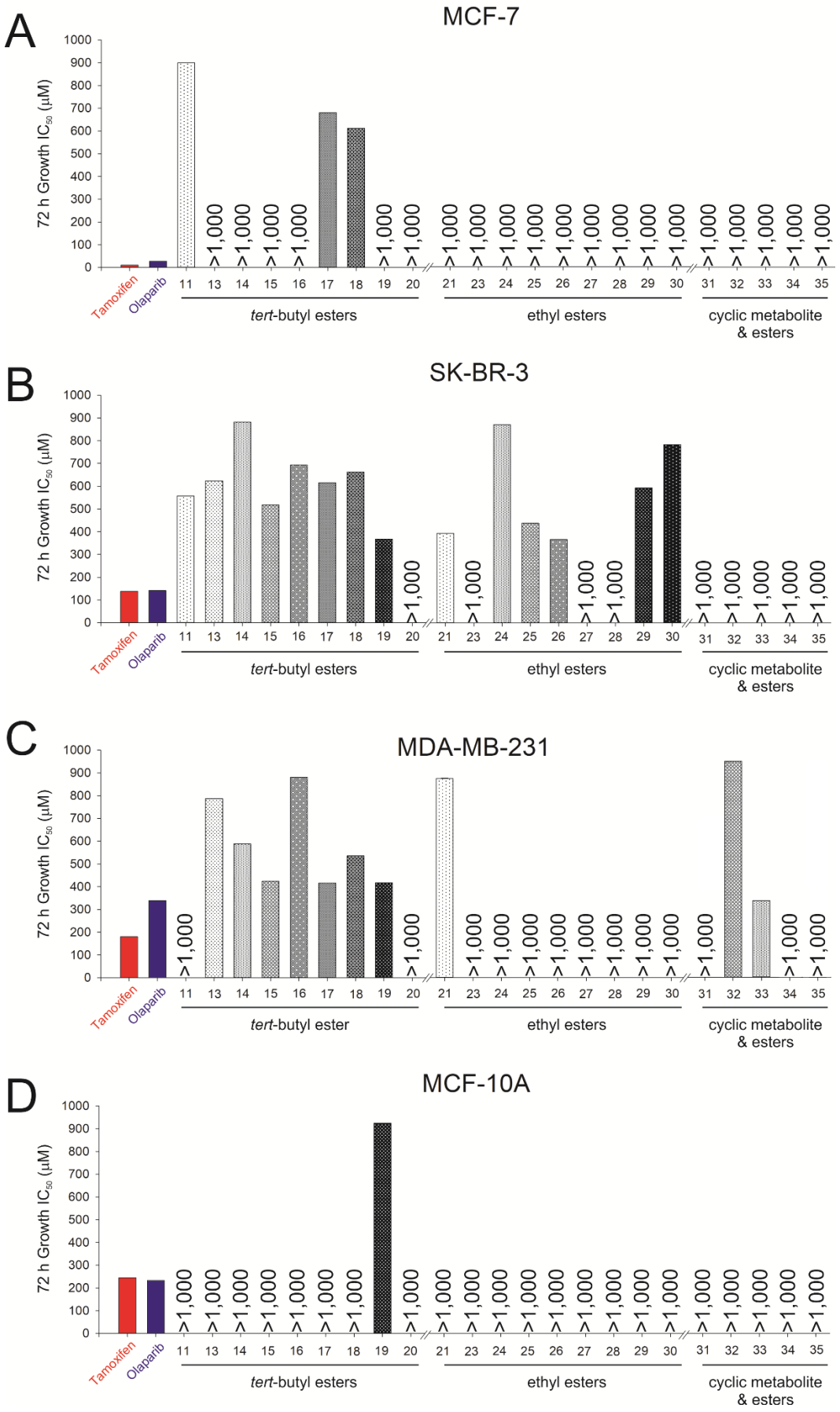

Figure 4. Effects of *tert*-butyl esters and ethyl esters of the *L*-γ-methyleneglutamic acid amides (**11**–**30**) and the cyclic metabolite and its *tert*-butyl esters and ethyl esters (**31** –**35**) on the inhibition of growth of breast cancer cells lines MCF-7, SK-BR-3, and MDA-MB-231 after 72 h of treatment. The nonmalignant MCF-10A breast cell line was used as a control.

2.4. Evaluation of the newly synthesized esters and the cyclic metabolite on inhibition of growth of breast cancer cells

The capacity for the *tert*-butyl esters and ethyl esters of the *L*-γ-methyleneglutamic acid amides (**11–30**) and the cyclic metabolite and its *tert*-butyl esters and ethyl esters (**31 –35**) to inhibit the growth of the three breast cancer cell lines MCF-7, SK-BR-3, and MDA-MB-231 was assessed after 72 h of treatment (**Figure 4**). The nonmalignant MCF-10A breast cell line was used as a control. The potencies of all newly synthesized compounds on MCF-7 or SK-BR-3 cell lines were markedly reduced compared to those of previously identified leads (**5**, **6**, or **9**; **Figure 2**), and none exhibited a significant increase in potency compared to tamoxifen or olaparib (positive controls) or were equipotent to compounds **5**, **6**, or **9**. Several *tert*-butyl esters of the *L*-γ-methyleneglutamic acid amides (**15**, **17**, and **19**) and *tert*-butyl ester of the cyclic metabolite (**33**) exhibited commensurate potencies to those of **5**, **6**, and **9** on the triple-negative MDA-MB-231 cells (**Figure 4C**); however, this cancer cell line exerted the strongest resistance to any compound evaluated. None of the compounds inhibited the growth of the nonmalignant MCF-10A breast cell line.

2.5. Evaluation of the newly synthesized esters and the cyclic metabolite for cytotoxic activity on breast cancer cells

Cell death for the *tert*-butyl esters and ethyl esters of the *L*-γ-methyleneglutamic acid amides (**11–30**) and the cyclic metabolite and its *tert*-butyl esters and ethyl esters (**31 –35**) on the three breast cancer cell lines MCF-7, SK-BR-3, and MDA-MB-231 was also assessed after 72 h of treatment (**Figure 5**). The nonmalignant MCF-10A breast cell line was used as a control. No compound exhibited significantly greater or equipotent effects to promote cancer cell death compared to **5**, **6**, or **9** on any breast cancer cell line. However, many compounds exerted greater toxicities on the nonmalignant MCF-10A breast cells than those observed for **5**, **6**, or **9** (see **13**, **14**, **16**, **18**, **20**, **21**, **23**, **24**, **26**, **27**, **29**, **30**, **33**, **34**; **Figure 5D**). Together, these data serve to highlight the beneficial profiles observed particularly in the *L*-γ-methyleneglutamic acid amides, which reduced the growth in MCF-7, SK-BR-3, and (to a lesser extent) MDA-MB-231 cells and promoted cancer cell death without producing toxicity in nonmalignant breast cells.

2.6 Pharmacokinetic parameters of the lead *L*-γ-methyleneglutamic acid amide (compound 5)

Given the promising *in vitro* profiles of the *L*-γ-methyleneglutamic acid amides, we carried out pharmacokinetic studies of the lead *L*-γ-methyleneglutamic acid amide (**5**) in male CD1 mice to determine its C_{max}, T_{max}, elimination half-life, mean clearance, and volume of distribution.

In plasma, the concentrations of **5** decreased mono-exponentially after 2.5 mg/kg *intravenous* administration. The mean clearance (CL) was found to be 29.4 mL/min/kg, which is ~31% of the hepatic blood flow in mice. The volume of distribution was found to be 4.6 L/kg. The terminal half-life ($t_{1/2}$) was 0.80 h (**Table 1**). Post-intraperitoneal administration, maximum plasma concentration (C_{max}: 1,543 ng/mL) was achieved at 0.22 h (T_{max}), indicating rapid absorption from gastrointestinal tract. The apparent half-life was 0.43 h, determined after intraperitoneal administration. The $AUC_{0-\alpha}$ attained post-intraperitoneal dose was 967 ng×h/mL. The absolute intraperitoneal bioavailability in mice at 2.5 mg/kg was 66%.

Post-intraperitoneal administration, maximum kidney concentration (C_{max}: 17,681 ng/g) was achieved at 0.50 h (T_{max}) (**Table 2**). The apparent half-life was 0.46 h. The $AUC_{0-\alpha}$ attained post-intraperitoneal dose was 21,944 ng×h/g. Maximum liver concentration (C_{max}: 7,291 ng/g) was achieved at 1 h (T_{max}). The apparent half-life was 0.43 h. The $AUC_{0-\alpha}$ attained post-intraperitoneal dose was 10,596 ng×h/g. Maximum brain concentration (C_{max}: 31 ng/g) was achieved at 0.5 h (T_{max}). The apparent half-life was 0.74 h. The

$AUC_{0-\alpha}$ attained post-intraperitoneal dose was 44 ng×h/g.

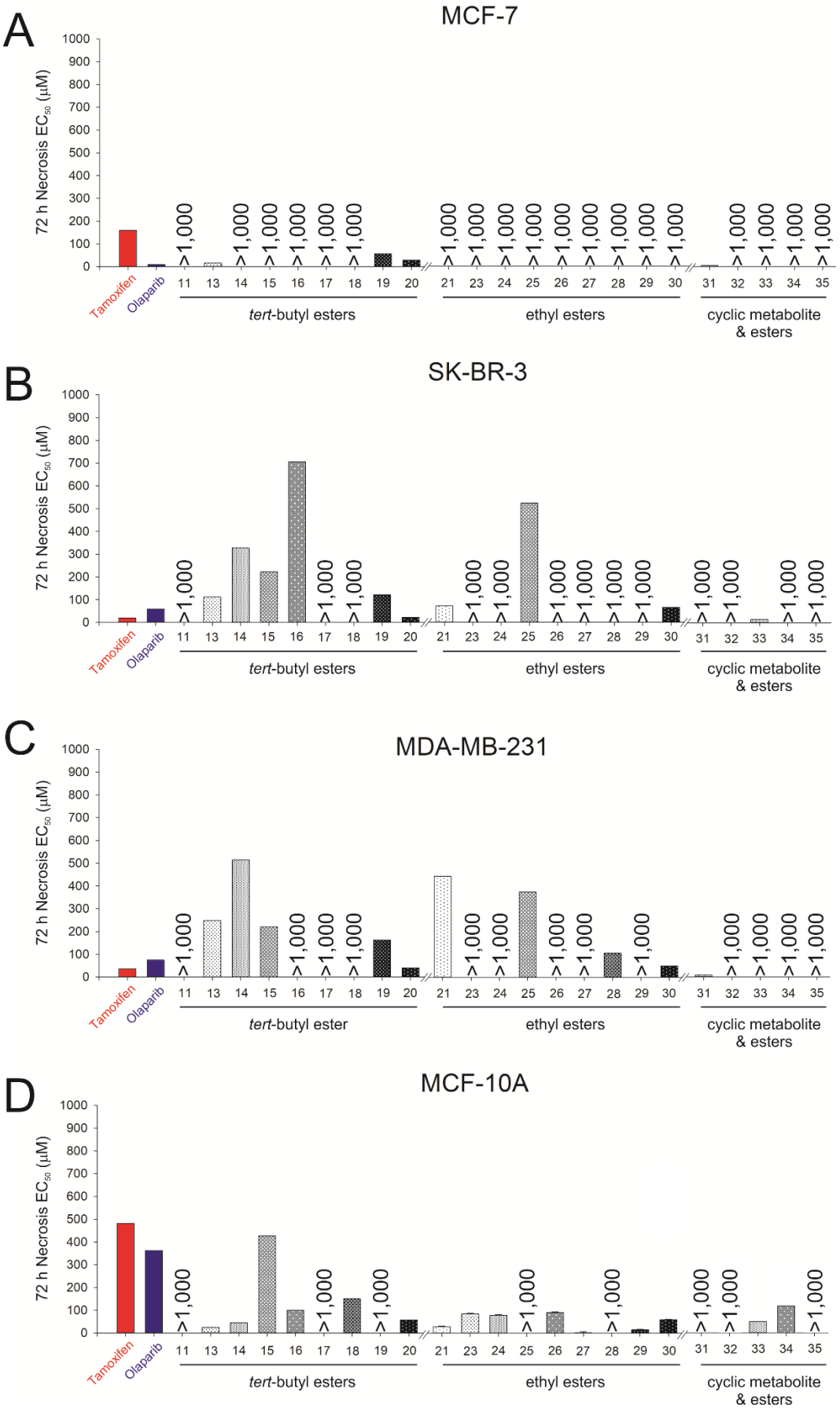

Figure 5. Effects of *tert*-butyl esters and ethyl esters of the *L*-γ-methyleneglutamic acid amides (**11**–**30**) and the cyclic metabolite and its *tert*-butyl esters and ethyl esters (**31** –**35**) on necrosis of breast cancer cells lines MCF-7, SK-BR-3, and MDA-MB-231 after 72 h of treatment. The nonmalignant MCF-10A breast cell line was used as a control.

Table 1. Pharmacokinetic parameters of the lead *L*-γ-methyleneglutamic acid amide (compound **5**) in the plasma of male CD1 mice after intravenous and intraperitoneal dosing to mice at 2.5 mg/kg.

PK parameters		Plasma	
		Intravenous	Intraperitoneal
$t_{1/2}$	h	0.80 ± 0.20	0.43 ± 0.12
C_0 or C_{max}	ng/mL	3,016 ± 819	1,543 ± 366
T_{max}	h	0.12 ± 0.04	0.22 ± 0.14
$AUC_{0-\alpha}$	ng×h/mL	1,457 ± 292	967 ± 349
F	%	---	66 ± 24

$t_{1/2}$: half-life; C_{max}: maximum concentration; T_{max}: time at maximum concentration; $AUC_{0-\alpha}$: area under the curve to infinite time; F: bioavailability.

Table 2. Pharmacokinetic parameters of the lead *L*-γ-methyleneglutamic acid amide (compound **5**) in the brain, kidney, and liver of male CD1 mice after intraperitoneal dosing to mice at 2.5 mg/kg.

PK parameters		Intraperitoneal		
		Brain	Kidney	Liver
$t_{1/2}$	h	0.74 ± 0.05	0.46 ± 0.04	0.43 ± 0.06
C_{max}	ng/g	31 ± 4	17,681 ± 4,577	7,291 ± 5,059
T_{max}	h	0.5 ± 0.0	0.5 ± 0.0	1 ± 0.5
$AUC_{0-\alpha}$	ng×h/g	44 ± 13	21,944 ± 1,531	10,596 ± 5,644

$t_{1/2}$: half-life; C_{max}: maximum concentration; T_{max}: time at maximum concentration; $AUC_{0-\alpha}$: area under the curve to infinite time.

2.7 Evaluation of the *L*-γ-methyleneglutamic acid amides on inhibition of growth of glioblastoma cells

Based on their selectivity and efficacy against breast cancer cell lines MCF-7, SK-BR-3, and MDA-MB-231,[11] compounds **3–9** were identified as our top 7 *L*-γ-methyleneglutamic acid amides. Since compound **5** showed moderate exposure to the brain with a half-life of 0.74 h, we decided to test the activity of the *L*-γ-methyleneglutamic acid amides **3–9** on glioblastoma cell lines BNC3 and BNC6. We found that they effectively suppressed the growth of these cancer cell lines after 24 or 72 h of treatment in a concentration-dependent manner (**Figure 6**). DMSO was used as the vehicle control, and BiCNU was used as a positive control. IC_{50} values of these compounds on inhibition of growth after 72 h of treatment are shown in **Table 3**.

2.8 Evaluation of the *L*-γ-methyleneglutamic acid amides on inhibition of growth of head and neck cancer cells

We also tested the activity of these compounds on head and neck cancer cell lines HN30 and HN31 and found that they effectively suppressed the growth of these cancer cell lines after 24 or 72 h of treatment in a concentration-dependent manner (**Figure 7**). DMSO was used as the vehicle control, and cisplatin was used as a positive control. IC_{50} values of these compounds on inhibition of growth after 72 h treatment are shown in **Table 3**.

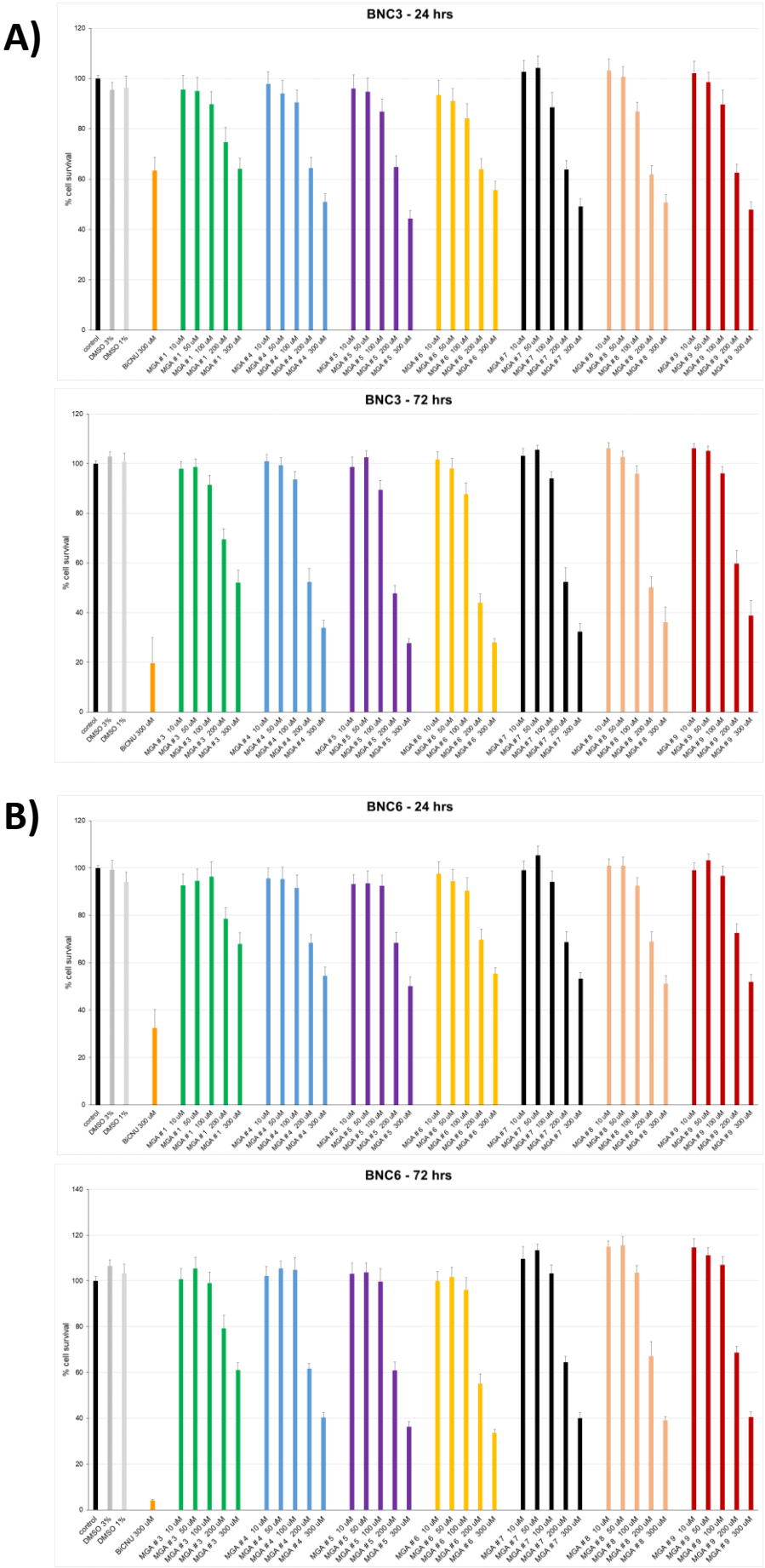

Figure 6. Effects of *L*-γ-methyleneglutamic acid amides (MGA) **3–9** on inhibition of growth glioblastoma cell lines BNC3 (**A**) and BNC6 (**B**) after 24 and 72 h of treatment. BiCNU was used as a positive control.

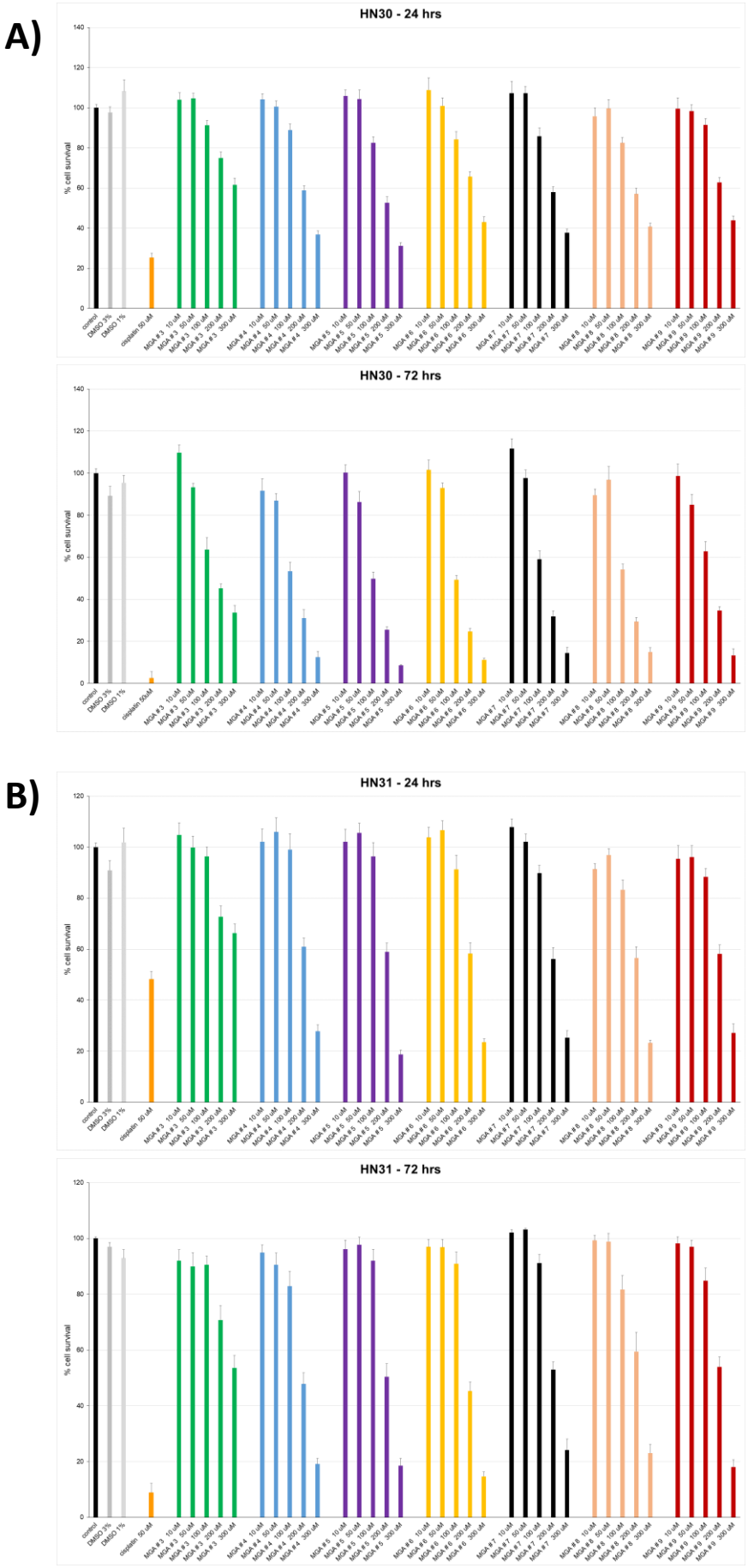

Figure 7. Effects of *L*-γ-methyleneglutamic acid amides (MGA) **3–9** on inhibition of growth of head and neck cancer cell lines HN30 (**A**) and HN31 (**B**) after 24 and 72 h of treatment. Cisplatin was used as a positive control.

Table 3. IC_{50} values (in μM) of *L*-γ-methyleneglutamic acid amides **3–9** on inhibition of growth of glioblastoma cell lines BNC3 and BNC6 and head and neck cancer cell lines HN30 and HN31 after 72 h of treatment.

Compound	IC_{50} ± SEM (μM)			
	BNC3	**BNC6**	**HN30**	**HN31**
BiCNU	156.7 ± 4.2	159.6 ± 4.4	ND	ND
cisplatin	ND	ND	10.5 ± 0.4	21.0 ± 0.4
3	217.5 ± 3.8	210.2 ± 4.6	92.9 ± 3.3	199.4 ± 4.3
4	170.9 ± 3.5	188.5 ± 3.4	119.4 ± 4.0	199.2 ± 3.7
5	169.0 ± 3.1	188.6 ± 4.1	102.1 ± 2.8	196.0 ± 3.5
6	156.4 ± 3.3	179.6 ± 3.8	91.8 ± 2.2	193.8 ± 2.9
7	171.4 ± 3.3	187.3 ± 3.4	105.4 ± 3.5	196.0 ± 2.2
8	158.2 ± 3.6	198.9 ± 3.5	97.0 ± 3.1	207.0 ± 3.9
9	181.7 ± 3.5	194.4 ± 3.2	219.6 ± 4.1	202.4 ± 3.1

ND: Not determined

3. Conclusion

Our lab recently discovered many *L*-γ-methyleneglutamic acid amides that were found to be as efficacious as tamoxifen or olaparib in inhibiting the growth of MCF-7, SK-BR-3, and MDA-MB-231 breast cancer cells after 24 or 72 h of treatment. None of the compounds inhibited the growth nor produce cytotoxicity on the nonmalignant MCF-10A breast cells. In this report, we synthesized and evaluated two series of *tert*-butyl ester and ethyl ester prodrugs of these *L*-γ-methyleneglutamic acid amides and the cyclic metabolite and its *tert*-butyl esters and ethyl esters on the three breast cancer cell lines MCF-7, SK-BR-3, and MDA-MB-231. The nonmalignant MCF-10A breast cell line was used as a control. These esters were found to also suppress the growth of the three breast cancer cell lines, but they were less potent compared to their parent *L*-γ-methyleneglutamic acid amides. As mentioned earlier, a possible target for these *L*-γ-methyleneglutamic acid amides is glutamine transporters, and these compounds would act as reversible inhibitors of glutamine transporters, rather than irreversible inhibitors. Recognizing that the ester group on these compounds might affect their binding to the glutamine transporters, we decided to keep the *N*-Boc group in these two newly synthesized ester series to see if we could enhance the availability of these compounds via membrane permeability, instead of glutamine transporters. The decrease in potency of these esters suggests that this is not a good approach and that the combination of *N*-Boc and ester groups would decrease the ability of glutamine transporters to transport these compounds. Two series of free amines and free carboxylic acids of these compounds are being synthesized and studied in our lab. Given the promising *in vitro* profiles of the *L*-γ-methyleneglutamic acid amides, we carried out pharmacokinetic studies of the lead *L*-γ-methyleneglutamic acid amide (**5**) in male CD1 mice to determine its C_{max}, T_{max}, elimination half-life, mean clearance, and volume of distribution. In general, this compound showed decent intraperitoneal bioavailability, moderate clearance, optimum half-life, and high volume of distribution. Notably, **5** displayed moderate exposure in the brain with a half-life of 0.74 h and good tissue distribution, such as in the kidney and liver. We then tested the top 7 *L*-γ-methyleneglutamic acid amides on glioblastoma cell lines BNC3 and BNC6 and head and neck cancer cell lines HN30 and HN31 and found that these compounds effectively suppressed the growth of these cancer cells after 24 or 72 h of treatment. Overall, the *L*-γ-methyleneglutamic acid amides hold promise as novel therapeutics for broad applications in anticancer therapy. Unlike many reported inhibitors of glutaminolysis,[9,10,24,25]

these *L*-*γ*-methyleneglutamic acid amides did not result in cytotoxicity in the nonmalignant MCF-10A breast cells. Specific targets of these compounds, especially in mitochondrial metabolism in cancer, are being studied to develop the next generations of novel anticancer agents.

4. Experimental Section

4.1. Chemistry

All chemicals were obtained from Sigma-Aldrich or Fisher Scientific and used as received, unless otherwise specified. All syntheses were conducted under anhydrous conditions and an argon atmosphere, using flame-dried glassware and employing standard techniques for handling air-sensitive materials, unless otherwise noted. All solvents were distilled and stored under an argon or nitrogen atmosphere before use. ^{1}H NMR and ^{13}C NMR spectra were recorded on a Bruker-400 or a Bruker-500 spectrometer using $CDCl_3$ or DMSO-d_6 as the solvent. Chemical shifts (δ) were recorded in parts per million (ppm) and referenced to $CDCl_3$ (7.26 ppm for ^{1}H NMR and 77.16 ppm for ^{13}C NMR) or DMSO-d_6 (2.50 ppm for ^{1}H NMR and 39.52 ppm for ^{13}C NMR). Coupling constants (*J*) are in Hz. The following abbreviations were used to designate the multiplicities: s = singlet, d = doublet, t = triplet, q = quartet, quint = quintuplet, m = multiplet, br = broad. LC-MS were measured with an ACQUITY-Waters micromass (ESCi) system. Exact high-resolution mass determinations were analyzed on a JEOL AccuToF 4G LCplus atmospheric pressure ionization time-of-flight mass spectrometer (Jeol, Tokyo, Japan) fitted with direct analysis in real-time (DART) ion source (IonSense DART controller, Saugus, MA, USA). The DART ion source was operated with helium gas (approximately 4.0 L/min flow rate), a gas heater (350 °C), and a source grid (350 V). The data acquisition range was from *m/z* 50 to 1000. Polyethylene glycol (PEG 600) was used for the exact mass calibration.

4.1.1. Syntheses of compounds 11 and 13–20

The syntheses of compounds **11** and **13–20** from *L*-pyroglutamic acid and their characterization were reported previously.[11]

4.1.2. Syntheses of compounds 21, 23–30, and 35

Ethyl (S)-5-oxopyrrolidine-2-carboxylate (45)

To a solution of *L*-pyroglutamic acid (**41**, 300 mg, 2.32 mmol) in ethanol (2.40 mL) under argon atmosphere was added conc. sulfuric acid (11.6 µL) dropwise and stirred for 24 h at room temperature. The reaction was quenched with an aqueous solution of sodium bicarbonate. Water was added to the reaction mixture, and the mixture was extracted with ethyl acetate (3 x 15 mL). The ethyl acetate layers were combined, dried with magnesium sulfate, and evaporated *in vacuo*. The crude mixture was purified by flash column chromatography with silica gel and hexanes/ethyl acetate to produce compound **45** (219 mg, 60% yield) as a viscous liquid. ^{1}H NMR (400 MHz, $CDCl_3$) δ 7.40 (s, 1H), 4.16 – 3.98 (m, 3H), 2.37 – 2.11 (m, 3H), 2.09 – 1.97 (m, 1H), 1.13 (td, *J* = 7.2, 0.8 Hz, 3H). ^{13}C NMR (101 MHz, $CDCl_3$) δ 178.4, 172.1, 61.2, 55.5, 29.2, 24.6, 13.9. HRMS calcd for $C_7H_{11}NO_3$ [M+H] 158.0817; found 158.0799.

1-(*tert*-Butyl) 2-ethyl (S)-5-oxopyrrolidine-1,2-dicarboxylate (46)

To a solution of compound **45** (539 mg, 3.40 mmol) in anhydrous dichloromethane (18.0 mL) were added DMAP (450 mg, 3.74 mmol), $(Boc)_2O$ (816 mg, 3.74 mmol), and Et_3N (570 µL) and stirred for 18 h at room temperature. Water was added to the reaction mixture, and the mixture was extracted with dichloromethane (3 x 20 mL). The dichloromethane layers were combined, dried with Na_2SO_4, and evaporated *in vacuo*. The crude product was purified by flash column chromatography with silica gel and hexanes/ethyl acetate to produce compound **46** (796 mg, 91% yield) as a white solid. ^{1}H NMR (400 MHz, $CDCl_3$) δ 4.18 (dd, *J* = 9.2, 2.9 Hz, 1H), 3.81 (q, *J* = 7.1 Hz, 2H), 2.21 – 1.91 (m, 3H), 1.65-1.54 (m, 1H),

1.05 (d, *J* = 1.6 Hz, 9H), 0.87 (dd, *J* = 7.7, 6.6 Hz, 3H). ^{13}C NMR (101 MHz, $CDCl_3$) δ 172.4, 170.5, 148.2, 82, 60.5, 58, 30.1, 26.8, 20.4, 13.2. HRMS calcd for $C_{12}H_{20}NO_5$ [M+H] 258.1341; found 258.1338.

1-(*tert*-Butyl) 2-ethyl (S)-4-methylene-5-oxopyrrolidine-1,2-dicarboxylate (35)

To a solution of compound **46** (300 mg, 1.17 mmol) in anhydrous THF (1.20 mL) was added 1M LiHMDS in THF (2.90 mL) dropwise and stirred for 30 min at -78 °C. To this reaction mixture, trifluoroethyl trifluoroacetate was added and stirred for 3.5 h at -78 °C. The reaction mixture was quenched with a saturated aqueous NH_4Cl solution and extracted with ethyl acetate (3 x 15 mL). The ethyl acetate layers were combined, dried with Na_2SO_4, and evaporated *in vacuo*. The crude product was used for the next step without purification. The crude product was dissolved in anhydrous benzene (9.0 mL), and K_2CO_3 (404 mg, 2.90 mmol), paraformaldehyde (351 mg, 11.7 mmol), and 18-crown-6 (42.4 mg, 10 mol%) were added. The reaction mixture was stirred at reflux for 4 h until the reaction was complete. The reaction was filtered, and the filtrate was concentrated. Water was then added, and the mixture was extracted with ethyl acetate (3 x 10 mL). The ethyl acetate layers were combined, dried with Na_2SO_4, and evaporated *in vacuo*. The crude product was purified by flash column chromatography with silica gel and hexanes/ethyl acetate to produce compound **35** (173 mg, 55% yield) as a sticky gel. ^{1}H NMR (400 MHz, $CDCl_3$) δ 6.13 (q, *J* = 2.7 Hz, 1H), 5.44 (q, *J* = 2.2 Hz, 1H), 4.57-4.49 (m, 1H), 4.21-4.07 (m, 2H), 3.07 – 2.94 (m, 1H), 2.67-2.57 (m, 1H), 1.47 – 1.38 (m, 9H), 1.21 – 1.14 (m, 3H). ^{13}C NMR (101 MHz, $CDCl_3$) δ 171.0, 165.5, 149.7, 136.6, 120.7, 83.6, 61.7, 55.7, 27.8, 27.7, 14.0. HRMS calcd for $C_{13}H_{20}NO_5$ [M+H] 270.1341; found 270.1338.

(S)-4-((*tert*-Butoxycarbonyl)amino)-5-ethoxy-2-methylene-5-oxopentanoic acid (47)

To a solution of compound **35** (89 mg, 0.33 mmol) in THF (3.50 mL) was added LiOH (15.83 mg, 0.66 mmol) and stirred for 18 h at room temperature. The reaction was quenched with a saturated aqueous solution of NH_4Cl and extracted with dichloromethane (3 x 5 mL). The dichloromethane layers were combined, dried with Na_2SO_4, and evaporated *in vacuo*. The crude product was purified by flash column chromatography with silica gel and dichloromethane/methanol to produce compound **47** (52 mg, 55% yield) as a sticky white solid. ^{1}H NMR (400 MHz, $CDCl_3$) δ 6.38 (s, 1H), 5.75 (s, 1H), 4.52 – 4.41 (m, 1H), 4.18 (q, *J* = 7.1 Hz, 2H), 2.83 (dd, *J* = 13.9, 5.6 Hz, 1H), 2.66 (dt, *J* = 22.1, 10.4 Hz, 1H), 1.42 (s, 9H), 1.27 (s, 3H). ^{13}C NMR (101 MHz, $CDCl_3$) δ 172.0, 170.8, 155.2, 135.4, 130.3, 79.9, 61.5, 52.9, 34.7, 28.2, 14.1. HRMS calcd for $C_{13}H_{22}NO_6$ [M+H] 288.1447; found 288.1436.

General procedure for amide coupling:

To a solution of the carboxylic acid (1.0 equiv) in anhydrous THF under argon atmosphere were added HBTU (1.5 equiv), Et_3N (1.5 equiv), 4-methylmorpholine (1.5 equiv), and amine (1.5 equiv) at room temperature. The reaction was stirred for about 3–4 h until completion (monitored using TLC) and then quenched with water. The reaction mixture was filtered, and the filtrate was concentrated *in vacuo* and purified by flash column chromatography with silica gel and hexanes/ethyl acetate or dichloromethane/methanol to produce the desired amide.

Ethyl (S)-2-((tert-butoxycarbonyl)amino)-4-carbamoylpent-4-enoate (21)

Compound **21** was synthesized from compound **47** (20 mg, 0.07 mmol) by following the general amide coupling procedure. Here, 4 equiv of ammonium chloride were used in the place of amine. Yield = 48% (9.6 mg). White solid. ^{1}H NMR (400 MHz, $CDCl_3$) δ 6.36 (s, 1H), 5.81 (s, 1H), 5.58 (s, 1H), 5.45 (s, 1H), 4.34 (q, *J* = 6.9 Hz,

1H), 4.18 (qd, *J* = 7.2, 1.6 Hz, 2H), 2.81 – 2.78 (m, 1H), 2.68 (dd, *J* = 14.0, 7.5 Hz, 1H), 1.42 (d, *J* = 1.2 Hz, 9H), 1.26 (td, *J* = 7.1, 1.5 Hz, 3H). ^{13}C NMR (101 MHz, $CDCl_3$) δ 171.7, 170.2, 155.6, 139.6, 122.9, 80.0, 61.5, 53.4, 35.5, 28.3, 14.2. HRMS calcd for $C_{13}H_{23}O_5N_2$ [M+H] 287.1606; found 287.1597.

Ethyl (S)-2-((tert-butoxycarbonyl)amino)-4-(phenylcarbamoyl)pent-4-enoate (23)

Compound **23** was synthesized from compound **47** (20 mg, 0.07 mmol) and aniline by following the general amide coupling procedure. Yield = 52% (13 mg). White solid. ^{1}H NMR (500 MHz, $CDCl_3$) δ 8.50 (s, 1H), 7.65 (d, *J* = 8.0 Hz, 2H), 7.41 – 7.31 (m, 2H), 7.13 (dd, *J* = 8.1, 6.5 Hz, 1H), 5.84 (s, 1H), 5.57 (d, *J* = 7.6 Hz, 1H), 5.46 (s, 1H), 4.40 (q, *J* = 7.1, 6.5 Hz, 1H), 4.20 (q, *J* = 7.2 Hz, 2H), 2.92 (dd, *J* = 14.0, 5.5 Hz, 1H), 2.73 (dd, *J* = 14.0, 7.7 Hz, 1H), 1.45 (s, 9H), 1.27 (td, *J* = 7.3, 1.6 Hz, 3H). ^{13}C NMR (126 MHz, $CDCl_3$) δ 171.6, 166.8, 155.9, 141.5, 138.2, 129.0, 124.5, 122.0, 120.2, 80.3, 61.8, 53.3, 36.4, 28.4, 14.3. HRMS calcd for $C_{19}H_{27}O_5N_2$ [M+H] 363.1919; found 363.1917.

Ethyl (S)-4-(benzylcarbamoyl)-2-((tert-butoxycarbonyl)amino)pent-4-enoate (24)

Compound **24** was synthesized from compound **47** (20 mg, 0.07 mmol) and benzylamine by following the general amide coupling procedure. Yield = 72% (19 mg). White solid. ^{1}H NMR (500 MHz, $CDCl_3$) δ 7.44 – 7.20 (m, 5H), 6.60 (s, 1H), 5.69 (s, 1H), 5.62 (d, *J* = 7.6 Hz, 1H), 5.38 (s, 1H), 4.51 (d, *J* = 5.6 Hz, 2H), 4.34 (q, *J* = 6.8 Hz, 1H), 4.17 (q, *J* = 7.1 Hz, 2H), 2.83 (dt, *J* = 15.8, 7.8 Hz, 1H), 2.74-2.66 (m, 1H), 1.42 (s, 9H), 1.26 (t, *J* = 7.2 Hz, 3H). ^{13}C NMR (126 MHz, $CDCl_3$) δ 171.9, 168.3, 155.7, 140.9, 138.2, 128.7, 127.9, 127.5, 121.5, 79.8, 61.4, 53.4, 43.9, 35.7, 28.4, 14.3. HRMS calcd for $C_{20}H_{29}O_5N_2$ [M+H] 377.2076; found 377.2067.

Ethyl (S)-2-((tert-butoxycarbonyl)amino)-4-((4-fluorobenzyl)carbamoyl)pent-4-enoate (25)

Compound **25** was synthesized from compound **47** (20 mg, 0.07 mmol) and 4-fluorobenzylamine by following the general amide coupling procedure. Yield = 70% (19 mg). White solid. ^{1}H NMR (500 MHz, $CDCl_3$) δ 7.35 – 7.18 (m, 2H), 7.08 – 6.92 (m, 2H), 6.88 – 6.73 (m, 1H), 5.71 (s, 1H), 5.66 – 5.54 (m, 1H), 5.37 (s, 1H), 4.44 (d, *J* = 5.8 Hz, 2H), 4.30 (q, *J* = 6.6 Hz, 1H), 4.15 (q, *J* = 7.1 Hz, 2H), 2.81 (dd, *J* = 14.2, 5.5 Hz, 1H), 2.66 (dd, *J* = 14.0, 7.3 Hz, 1H), 1.40 (d, *J* = 2.4 Hz, 9H), 1.24 (t, *J* = 7.1 Hz, 3H). ^{13}C NMR (126 MHz, $CDCl_3$) δ 171.7, 168.1, 163.2, 161.2, 155.6, 140.6, 133.9, 129.6, 121.7, 115.6, 115.4, 80.0, 61.5, 53.3, 43.1, 35.6, 28.3, 14.2. ^{19}F NMR (471 MHz, $CDCl_3$) δ -115.2. HRMS calcd for $C_{20}H_{28}O_5N_2F_1$ [M+H] 395.1982; found 395.1975.

Ethyl (S)-2-((tert-butoxycarbonyl)amino)-4-((4-nitrobenzyl)carbamoyl)pent-4-enoate (26)

Compound **26** was synthesized from compound **47** (20 mg, 0.07 mmol) and 4-nitrobenzylamine by following the general amide coupling procedure. Yield = 75% (22 mg). White solid. ^{1}H NMR (400 MHz, $CDCl_3$) δ 8.22 – 8.16 (m, 2H), 7.54 – 7.49 (m, 2H), 5.84 (s, 1H), 5.51 (s, 1H), 4.68 – 4.52 (m, 2H), 4.40 – 4.27 (m, 1H), 4.23-4.14 (m, 2H), 2.84 (dd, *J* = 14.0, 5.6 Hz, 1H), 2.71 (dd, *J* = 14.1, 7.9 Hz, 1H), 1.43 (s, 9H), 1.27 (td, *J* = 7.2, 2.1 Hz, 4H). ^{13}C NMR (101 MHz, $CDCl_3$) δ 170.8, 167.8, 154.7, 145.6, 144.8, 138.5, 126.6, 122.6, 120.8, 78.7, 60.3, 52.2, 41.6, 33.5, 26.7, 12.5. HRMS calcd for $C_{20}H_{28}O_7N_3$ [M+H] 422.1927; found 422.1922.

Ethyl (S)-2-((tert-butoxycarbonyl)amino)-4-(cyclopropylcarbamoyl)pent-4-enoate (27)

Compound **27** was synthesized from compound **47** (20 mg, 0.07 mmol) and cyclopropylamine by following the general amide coupling procedure. Yield = 60% (14 mg). Off-white solid. ^{1}H NMR (500 MHz, $CDCl_3$) δ 6.60 (s, 1H), 5.62 (d, *J* = 8.5 Hz, 1H), 5.32 (s, 1H), 4.25 (q, *J* = 6.8 Hz, 1H), 4.19-4.11 (m, 2H), 2.77 – 2.71 (m, 2H), 2.64 (dd, *J* = 14.0, 7.4 Hz, 1H), 1.40 (s, 9H), 1.24 (t, *J* = 7.2

Hz, 3H), 0.81 – 0.71 (m, 2H), 0.58 – 0.51 (m, 2H).^{13}C NMR (126 MHz, $CDCl_3$) δ 171.8, 169.8, 155.7, 140.7, 121.5, 80.0, 61.6, 53.6, 35.5, 28.4, 23.0, 14.3, 6.5. HRMS calcd for $C_{16}H_{27}O_5N_2$ [M+H] 327.1919; found 327.1912.

Ethyl (S)-2-((tert-butoxycarbonyl)amino)-4-(piperidine-1-carbonyl)pent-4-enoate (28)

Compound **28** was synthesized from compound **47** (20 mg, 0.07 mmol) and piperidine by following the general amide coupling procedure. Yield = 55% (14 mg). Sticky gel. ^{1}H NMR (500 MHz, $CDCl_3$) δ 5.63 (d, *J* = 8.1 Hz, 1H), 5.23 (d, *J* = 1.4 Hz, 1H), 5.10 (s, 1H), 4.25 (td, *J* = 7.7, 4.7 Hz, 1H), 4.15-4.07 (m, 2H), 3.53 – 3.40 (m, 4H), 2.80 – 2.57 (m, 2H), 1.63-1.56 (m, 2H), 1.50 (m, 4H), 1.36 (s, 9H), 1.20 (t, *J* = 7.2 Hz, 3H). ^{13}C NMR (126 MHz, $CDCl_3$) δ 171.8, 169.8, 155.5, 139.5, 118.3, 79.6, 61.3, 53.1, 48.3, 42.7, 36.1, 28.3, 24.6, 14.2. HRMS calcd for $C_{18}H_{31}O_5N_2$ [M+H] 355.2232; found 355.2225.

Ethyl (S)-2-((tert-butoxycarbonyl)amino)-4-((4-fluorophenyl)carbamoyl)pent-4-enoate (29)

Compound **29** was synthesized from compound **47** (20 mg, 0.07 mmol) and 4-fluoroaniline by following the general amide coupling procedure. Yield = 43% (11 mg). White solid. ^{1}H NMR (400 MHz, $CDCl_3$) δ 8.59 (s, 1H), 7.62 (dd, *J* = 8.4, 4.6 Hz, 2H), 7.10 – 6.94 (m, 2H), 5.85 (s, 1H), 5.57 – 5.37 (m, 2H), 4.36 (q, *J* = 7.0 Hz, 1H), 4.19 (d, *J* = 7.2 Hz, 2H), 2.90 (dd, *J* = 14.1, 6.0 Hz, 1H), 2.75 – 2.69 (m, 1H), 1.43 (s, 9H), 1.27 (d, *J* = 7.0 Hz, 3H). ^{13}C NMR (101 MHz, $CDCl_3$) δ 171.5, 166.4, 160.6, 158.2, 155.9, 141.1, 121.9, 115.8, 115.4, 80.4, 61.8, 53.2, 36.6, 28.3, 14.1. ^{19}F NMR (377 MHz, $CDCl_3$) δ -118.1. HRMS calcd for $C_{19}H_{26}O_5N_2F_1$ [M+H] 381.1825; found 381.1813.

Ethyl (S)-2-((tert-butoxycarbonyl)amino)-4-((4-chlorophenyl)carbamoyl)pent-4-enoate (30)

Compound **30** was synthesized from compound **47** (20 mg, 0.07 mmol) and 4-chloroaniline by following the general amide coupling procedure. Yield = 40% (11 mg). Off-white solid. ^{1}H NMR (400 MHz, $CDCl_3$) δ 8.66 (s, 1H), 7.63 (d, *J* = 8.4 Hz, 2H), 7.33 – 7.27 (m, 2H), 5.87 (s, 1H), 5.46 (d, *J* = 9.6 Hz, 2H), 4.36 (q, *J* = 6.9 Hz, 1H), 4.19 (q, *J* = 7.1 Hz, 2H), 2.98 – 2.84 (m, 1H), 2.71 (dd, *J* = 14.0, 7.2 Hz, 1H), 1.44 (s, 9H), 1.26 (t, *J* = 7.1 Hz, 3H). ^{13}C NMR (101 MHz, $CDCl_3$) δ 171.4, 166.3, 155.9, 140.9, 136.9, 129.3, 128.9, 122.8, 121.3, 80.5, 61.9, 53.1, 36.7, 28.3, 14.2. HRMS calcd for $C_{19}H_{26}O_5N_2Cl_1$ [M+H] 397.1530; found 397.1507.

4.1.3. Synthesis of compounds 31–34

(S)-4-Methylene-5-oxopyrrolidine-2-carboxylic acid (31)

To a solution of compound **33** (15 mg, 0.05 mmol) in dichloromethane (1.25 mL) were added trifluoroacetic acid (1.25 mL) and anisole (54 μL) and stirred at room temperature. The reaction progress was monitored using TLC and continued until full consumption of **33**. The reaction mixture was then evaporated and purified by flash column chromatography with silica gel and dichloromethane/methanol to produce compound **31** (7.0 mg, 98% yield) as a sticky gel. ^{1}H NMR (400 MHz, DMSO) δ 8.47 (s, 1H), 5.71 (td, *J* = 2.7, 1.2 Hz, 1H), 5.33 (tt, *J* = 2.2, 1.2 Hz, 1H), 4.17 – 4.10 (m, 1H), 3.14-3.04 (m, 1H), 2.72 (dq, *J* = 17.6, 2.8 Hz, 1H). ^{13}C NMR (101 MHz, DMSO) δ 174.4, 169.5, 139.6, 115.1, 52.1, 30.6. HRMS calculated for $C_6H_6O_3N_1$ [M-H] 140.0348; found 140.0405.

tert-Butyl (S)-4-methylene-5-oxopyrrolidine-2-carboxylate (32)

To a solution of compound **33** (30 mg, 0.10 mmol) in acetonitrile (3.0 mL) were added a few drops of 3M HCl and stirred at room temperature. The reaction progress was monitored using TLC and continued until full consumption of **33**. The reaction was then quenched with a saturated solution of sodium bicarbonate and extracted with ethyl acetate (3 x 5 mL). The ethyl acetate layers were combined, dried with $MgSO_4$, and purified by flash column chromatography with silica gel and dichloromethane/methanol to produce compound

32 (17 mg, 85 % yield) as a sticky gel. ^{1}H NMR (400 MHz, $CDCl_3$) δ 6.50 (s, 1H), 6.03 (t, *J* = 2.8 Hz, 1H), 5.40 (q, *J* = 1.9 Hz, 1H), 4.18-4.12 (m, 1H), 3.18-3.07 (m, 1H), 2.97-2.87 (m, 1H), 1.47 (s, 9H). ^{13}C NMR (101 MHz, $CDCl_3$) δ 170.5, 169.9, 137.2, 117.0, 82.7, 53.0, 30.2, 28.0. HRMS calcd for $C_{10}H_{16}NO_3$ [M+H] 198.1130; found 198.1135.

Di-tert-butyl (S)-4-methylene-5-oxopyrrolidine-1,2-dicarboxylate (**33**)

Compound **33** was synthesized by following our previously reported method (**Scheme 1**).[11] To a solution of *L*-pyroglutamic acid (**41**, 1.00 g, 7.73 mmol) in *tert*-butyl acetate (10.0 mL) was added 70% perchloric acid (230 µL) and stirred for 18 h at room temperature. The reaction was quenched with a saturated solution of sodium bicarbonate and extracted with diethyl ether (3 x 25 mL). The diethyl ether layers were combined and evaporated *in vacuo*. The crude extract was purified by flash chromatography with silica gel and hexanes/ethyl acetate to produce compound **42**, which was used in the next step.

To a solution of compound **42** (500 mg, 2.70 mmol) in dichloromethane (15.0 mL) were added di-*tert*-butyl dicarbonate (682 µL, 2.97 mmol), triethylamine (413 µL, 2.97 mmol), and 4-dimethylaminopyridine (363 mg, 2.97 mmol) and stirred for 18 h at room temperature. Water was added to the reaction mixture, and the mixture was extracted with dichloromethane (3 x 20 mL). The dichloromethane layers were combined and evaporated *in vacuo*. The crude extract was then purified by flash column chromatography with silica gel and hexanes/ethyl acetate to produce compound **43** (1.92 g, 87% yield) as a viscous liquid. ^{1}H NMR (400 MHz, $CDCl_3$) δ 4.37 (dp, *J* = 8.7, 2.2 Hz, 1H), 2.55 – 2.42 (m, 1H), 2.42 – 2.28 (m, 1H), 2.27-2.12 (m, 1H), 1.94-1.82 (m, 1H), 1.42-1.34 (m, 18H).^{13}C NMR (101 MHz, $CDCl_3$) δ 173.4, 170.3, 149.1, 83.0, 82.0, 59.5, 31.0, 27.79, 27.76, 21.5. ^{1}H and ^{13}C NMR spectra matched with those previously reported.[11]

Compound **43** (400 mg, 1.40 mmol) was dissolved in anhydrous THF (1.4 mL) under an argon atmosphere and cooled to -78 °C. 1M solution of LiHMDS in THF (3.5 mL, 3.5 mmol) was added to the reaction mixture dropwise and stirred for 30 min at -78 °C. 2,2,2-Trifluoroethyl trifluoroacetate (220 µL, 1.68 mmol) was added to the reaction mixture and stirred for 3.5 h at -78°C. The reaction mixture was quenched with an aqueous solution of ammonium chloride and extracted with dichloromethane (3 x 10 mL). The dichloromethane layers were combined, dried with sodium sulfate, evaporated *in vacuo*, and used in the next step without purification. The crude intermediate product was dissolved in anhydrous benzene (13.0 mL). Potassium carbonate (484 mg, 3.50 mmol), paraformaldehyde (420 mg, 14 mmol), and 18-crown-6 (55.5 mg, 0.21 mmol) were added under argon atmosphere, and the reaction mixture was stirred at reflux for 4 h. The reaction mixture was filtered, and the filtrate was evaporated and purified by flash column chromatography with silica gel and hexanes/ethyl acetate to produce compound **33** (312 mg, 75% yield) as a viscous colorless gel. ^{1}H NMR (400 MHz, $CDCl_3$) δ 6.22 (t, *J* = 2.8 Hz, 1H), 5.50 (t, *J* = 2.5 Hz, 1H), 4.48 (dd, *J* = 10.1, 3.1 Hz, 1H), 3.14 – 2.96 (m, 1H), 2.68 (dt, *J* = 3.3, 2.3 Hz, 1H), 1.46 (s, 18H). ^{13}C NMR (101 MHz, $CDCl_3$) δ 169.9, 165.5, 149.7, 136.8, 120.3, 83.3, 82.2, 56.3, 27.8. ^{1}H and ^{13}C NMR spectra matched with those previously reported.[11]

Ethyl (S)-4-methylene-5-oxopyrrolidine-2-carboxylate (34)

To a solution of compound **35** (25 mg, 0.09 mmol) in acetonitrile (3.0 mL) were added a few drops of 3M HCl and stirred at room temperature. The reaction was monitored using TLC and continued until full consumption of the starting material. The reaction was quenched with a saturated solution of sodium bicarbonate and extracted with ethyl acetate (3 x 5 mL). The ethyl acetate layers were combined, dried with $MgSO_4$, and purified by flash column chromatography with silica gel and

dichloromethane/methanol to produce compound **34** (10 mg, 66% yield) as a sticky gel. ^{1}H NMR (400 MHz, CDCl3) δ 6.38 (s, 1H), 6.08 (t, *J* = 2.8 Hz, 1H), 5.45 (q, *J* = 3.6, 2.6 Hz, 1H), 4.32 – 4.20 (m, 3H), 3.26-3.16 (m, 1H), 3.06-2.95 (m, 1H), 1.32 (t, *J* = 7.1 Hz, 3H). ^{13}C NMR (101 MHz, CDCl3) δ 171.4, 169.7, 136.7, 117.4, 61.9, 52.3, 30.2, 14.1. HRMS calcd for $C_8H_{12}NO_3$ [M+H] 170.0817; found 170.0827.

4.2. Evaluation of the *tert*-butyl esters and ethyl esters of the *L*-γ-methyleneglutamic acid amides and the cyclic metabolite and its *tert*-butyl esters and ethyl esters on the inhibition of growth and cytotoxic activity of breast cancer cells

All cell lines were purchased from the American Type Culture Collection (ATCC; Manassas, VA) and cultured according to the manufactured protocol. All cells were used between 2 and 5 passages. Cells were seeded on 96-well plates at a density of 2×10^4 cells per well for the assessment of live/dead assay. MCF-7, SK-BR-3, and MDA-MB-231 cells were maintained in DMEM/F12 media (#11320-033, Life Technologies, Carlsbad, CA) supplemented with 10% heat-inactivated fetal bovine serum (FBS; #SH30071.03, Thermo Scientific Hyclone, Logan, UT) and 0.5% antibiotic/antimycotic mixture (#15240-062, Life Technologies). MCF-10A cells were maintained in MEBM growth media supplemented with all components of a MEGM kit (#CC-3150, Lonza Group Ltd, Switzerland), with exception of #GA-1000 (gentamycin–amphotericin-B mixture). In addition, 0.5% penicillin-streptomycin mixture (#15-140-163, Thermo Fisher Scientific, Waltham, MA) and Cholera toxin (100 ng /mL; #C8052, Sigma) were added to the media. All compounds were dissolved in 50% DMSO, except tamoxifen which was dissolved in 90% EtOH. All compounds were then diluted to concentration in media (DMSO final concentration < 0.8%; EtOH final concentration < 0.6%). Control cells were incubated with the same concentrations of DMSO or EtOH and used as a negative control for statistical comparison. Cells were incubated with all compounds in a concentration-response regimen (0.32, 1, 3.2, 10, 32, 100, 320 μM) for either 24 or 72 h at 37 °C in tissue culture incubator (5% CO_2). The media were not changed during the experiment. On the day of assessment, a working solution of propidium iodide **($^{ex}/_{em}$: $^{536}/_{617}$ nm)** and Hoechst 33342 **($^{ex}/_{em}$: $^{350}/_{461}$ nm)** was prepared by diluting stocks in Hank's Balanced Salt Solution (HBSS; 1: 50 dilution for propidium iodide and 1/10 000 for Hoescht). Propidium iodide is a membrane-impermeable dye that only identifies cells wherein the cytoplasmic membrane has been disrupted (i.e. necrotized); as such, it is an unambiguous measure of cell death. At the end of incubation, media in the 96-well plates were removed and 100 μL of HBSS containing fluorophores was added to each well. Cells were incubated for 15 min at 37 °C (5% CO_2), and fluorescent emissions were read on a CLARIOstar plate reader (BMG Labtech, Cary, NC). Relative fluorescent units (RFU) for treatment wells were calculated as a proportion of untreated control wells to assess growth (negative controls are indicated by the dashed line at 100% in **Figure 4**). The viability of the cells was assessed by calculating the proportion of necrotic cells as a function of the total cell RFU per well (data are depicted as a % increase from negative control wells in **Figure 5**). All experiments were independently replicated 3 times, and each treatment was run in technical duplicate for each experiment.

4.3. Statistical analyses

To delineate differences in cell growth and necrosis in comparison to negative controls (vehicle-treated cells), separate two-way analyses of variance (ANOVA) were conducted with treatment exposure time (24 or 72 h) and compound concentration as the between-subjects factors. For each compound, simple main effects and planned *post hoc* contrasts were conducted to reveal dosing that differed significantly from controls. All *post hoc* comparisons were corrected for family-wise error and considered significant

when $p \leq 0.05$. To assess comparative changes in potency from positive controls (tamoxifen and olaparib), median inhibitory and effective concentrations ($\log IC_{50}$, $\log EC_{50}$) were determined *via* nonlinear regression (sigmoidal curvilinear modeling with a variable slope; Prism 7, GraphPad Software, La Jolla, CA) using a least-squares fit for each treatment group (bottom values constrained to 0). For each cell type (MCF-7, SK-BR-3, MDA-MB-231, or MCF-10A) and treatment time (24 or 72 h), $\log IC_{50}$ or $\log EC_{50}$ values were compared to those obtained for tamoxifen and olaparib *via* extra sum-of-squares *F*-test. Median shifts were considered significant when $p \leq 0.05$.

4.4. Pharmacokinetic studies of the lead *L*-γ-methyleneglutamic acid amide (compound 5)

Preparation of stock solutions, calibration standards, quality control samples, and the internal standard solution:

The primary stock solutions of compound **5** and tolbutamide (internal standard, IS) were prepared in methanol at a concentration of 1.0 mg/mL. Working solutions of calibration standards and quality control (QC) samples were prepared by dilution with acetonitrile:DMSO (9:1, v/v) and stored at -20 ˚C. A working stock of the IS solution (20 ng/mL) was prepared in methanol and stored at -20 ˚C.

Instruments and analytical conditions:

Chromatography was performed on an Acquity™ UPLC system (Waters Corp., Milford, MA) with an autosampler at the temperature of 10 °C. Waters Acquity UPLC® HSS C18 column (3.0×50 mm, 1.8 µm particle size) was used for chromatographic separation with linear gradient elution consisting of (A) 90% acetonitrile and (B) 10% of 0.2% formic acid in Milli-Q water as the mobile phase. The flow rate was set at 0.30 mL/min, and the injection volume was 2 µL.

An Acquity Tandem Quadrupole Mass Detector (Xevo TQ-S; Waters Corp, Milford, MA) in positive electrospray ionization mode was used for mass spectrometric detection. For collision-induced dissociation, argon was used as collision gas. The cone voltage and collision energy were set at 40 V and 20 V for compound **5** and 46 V and 26 V for the IS, respectively. Quantification was performed using multiple reaction monitoring (MRM) of the following transitions: m/z 267.1/108.9 for compound **5** and m/z 271.1/90.9 for IS. The retention times of compound **5** and IS were 1.40 and 2.12 min, respectively. The run time was 3.0 min.

Sample preparation:

A simple protein precipitation method was followed for the extraction of compound **5** from mouse plasma. To an aliquot of 50 µL of plasma or tissue (brain, liver, or kidney) samples, IS solution (5 µL of 20 ng/mL) was added and mixed for 15 sec on a cyclomixer (Thermo Scientific, IN, USA). After precipitation with 200 µL of acetonitrile, the mixture was vortexed for 2 min, followed by centrifugation for 10 min at 14,000 rpm on an accuSpin Micro 17R (Fisher Scientific, USA) at 5 °C. An aliquot of ~150 µL of clear supernatant was transferred into vials, and 2 µL was injected into the LC-MS/MS system for analysis.

In vivo study in CD1 mice:

Male CD1 mice were quarantined in the animal house of the University of Mississippi for 7 days with a 12 h dark/light cycle, and they had free access to standard pellet feed and water during this period. The protocols of the animal experiments were submitted to the Committee for the Purpose of Control and Supervision of Experimentation on Animals and were approved by the Institutional Animal Ethics Committee. For all experimental work, the animals were kept on a ~4 h fasting and had access to water *ad libitum*. Feed was provided 2 h post compound administration, and water was allowed *ad libitum*.

Following a ~4 h fasting, animals were divided into two groups. Group I and II animals (n = 24 for each study, weight range 25–30 g) were dosed with compound **5** intraperitoneally and *intravenously* (using a solution formulation comprising 5% DMSO and 95% normal saline) at a 2.5 mg/kg dose, respectively. At each time point post-dosing, the animals were sacrificed, and blood samples were drawn into polypropylene tubes containing K_2.EDTA solution as an anticoagulant at pre-dose, 0.083, 0.5, 1, 2, 4, 8, and 24 h. For the intraperitoneal administration group, tissue samples (brain, liver, or kidney) were collected at pre-dose, 0.5, 2, 4, and 24 h, respectively.

Plasma was harvested by centrifuging the blood using Eppendorf 5430R Centrifuge (Germany) at 5,000 rpm for 5 min and stored frozen at -80 ± 10 °C until analysis. Following the collection of brain, liver, or kidney tissues in a separate 15 mL round-bottom screw-capped vial, phosphate-buffered saline (5 volumes of each tissue weight) was added and homogenated with a homogenizer (Polytron®) and stored at -80 ± 10 °C until analysis. Plasma or tissue homogenate (50 µL) samples were spiked with IS and processed as mentioned in the sample preparation section.

Plasma or tissue concentration-time data of compound **5** were analyzed by noncompartmental analysis using WinNonlin Version 5.3 (Pharsight Corporation, Mountain View, CA, USA).

4.5 Evaluation of the *L*-γ-methyleneglutamic acid amides on the inhibition of growth of glioblastoma cells

Primary human glioblastoma (GBM) cell lines BNC3 and BNC6 were derived from surgical tissue resection obtained according to Marshall University tissue procurement IRB protocol #326290. BNC cancer cell lines were maintained in RPMI 1640 medium (HyClone, Thermo-Scientific) supplemented with 10% fetal bovine serum (FBS) (Thermo Fisher, Waltham, MA) and penicillin-streptomycin solution (penicillin 100 IU/mL, streptomycin 100 µg/mL, Corning, Cellgro, Manassas, VA). Cells were grown in a 37 °C humidified incubator supplemented with 5% CO_2.

Cell survival assay:

Glioblastoma cells were seeded at 3,000 cells/well in a 384-well plate format. After 24 h, cells were treated with compounds at doses of 10, 50, 100, 200, and 300 µM for 24 or 72 h. BiCNU was used as the control. Inhibition of growth was determined by adding Cell Counting Kit-8 (CCK8, APExBio, Houston, TX). After 2 h of incubation at 37 °C, optical density was measured at 450 nm using a SpectraMax M3 spectrophotometer (Molecular Devices, San Jose, CA). Results are expressed as percentages of cell survival. All experiments were independently replicated 3 times.

4.6 Evaluation of the *L*-γ-methyleneglutamic acid amides on the inhibition of growth of head and neck cancer cells

Radiotherapy-resistant, human HNSCC cell lines HN30 (derived from pharynx SCC– Stage T3) and HN31 (derived from a lymph node metastasis of the same patient) were gifts from Dr. George Yoo (Karmanos Cancer Center, Wayne State University, OH).[26,27] HNSCC cancer cell lines were maintained in RPMI 1640 medium (HyClone, Thermo-Scientific) supplemented with 10% fetal bovine serum (FBS) (Thermo Fisher, Waltham, MA) and penicillin-streptomycin solution (penicillin 100 IU/mL, streptomycin 100 µg/mL, Corning, Cellgro, Manassas, VA). Cells were grown in a 37 °C humidified incubator supplemented with 5% CO_2.

Cell survival assay:

Head and neck cancer cells were seeded at 3,000 cells/well in a 384-well plate format. After 24 h, cells were treated with compounds at doses of 10, 50, 100, 200, and 300 µM for 24 or 72 h. Cisplatin was used as the control. Inhibition of growth was determined by adding Cell Counting Kit-8 (CCK8,

APExBio, Houston, TX). After 2 h of incubation at 37 °C, optical density was measured at 450 nm using a SpectraMax M3 spectrophotometer (Molecular Devices, San Jose, CA). Results are expressed as percentages of cell survival. All experiments were independently replicated 3 times.

ASSOCIATED CONTENT

Supporting Information

Log(IC_{50}) and Log(EC_{50}) values on inhibition of growth and necrosis, respectively, of MCF-7, SK-BR-3, MDA-MB-231, and MCF-10A, and NMR spectra information. Supporting Information can be found online at https://www.sciencedirect.com/

AUTHOR CONTRIBUTIONS

M.I.H.K., M.I.H., and T.T. synthesized, purified, and characterized the *tert*-butyl esters and ethyl esters of the *L*-γ-methyleneglutamic acid amides. M.I.H.K., N.S.A., and T.T. synthesized, purified, and characterized the cyclic metabolite and its *tert*-butyl esters and ethyl esters. A.T.A. carried out the initial syntheses and characterization of the ethyl esters of the cyclic metabolite. S.J.K measured the HRMS for all synthesized compounds. F.M. and J.J.P. evaluated the *tert*-butyl esters and ethyl esters of the *L*-γ-methyleneglutamic acid amides and the cyclic metabolite and its *tert*-butyl esters and ethyl esters for their antigrowth/necrotic activity on breast cancer cells. S.P.S. and C.T. performed the pharmacokinetic study of the lead *L*-*γ*-methyleneglutamic acid amide (compound **5**). P.P. and P.P.C. carried out the evaluation of the *L*-*γ*-methyleneglutamic acid amides for their antigrowth activity on glioblastoma cells and head and neck cancer cells. H.V.L. designed the molecules and supervised the overall coordination of the research. M.I.H.K, J.J.P., and H.V.L. wrote the manuscript. M.I.H.K., F.M., P.P., S.J.K., S.P.S., P.P.C., J.J.P., and H.V.L. participated in the revision, and all authors approved the final version of the manuscript.

CONFLICTS OF INTEREST

The authors declare no conflict of interest.

ACKNOWLEDGMENT

Work was supported by the American Association of Colleges of Pharmacy (2018 New Investigator Award to H.V.L.), NIH (R00 DA039791 to J.J.P.; P30GM122733 pilot project awards to H.V.L. and J.J.P.), and funds from the Department of BioMolecular Sciences at the University of Mississippi School of Pharmacy. The content is solely the responsibility of the authors and does not necessarily represent the official views of these funders.

REFERENCES

(1) World Health Organization. Breast Cancer - Fact Sheet https://www.who.int/news-room/fact-sheets/detail/breast-cancer (accessed Mar 1, 2022).

(2) Mariniello, G.; Peca, C.; Del Basso De Caro, M.; Carotenuto, B.; Formicola, F.; Elefante, A.; Maiuri, F. Brain Gliomas Presenting with Symptoms of Spinal Cord Metastasis. *Neuroradiol. J.* **2015**, *28* (5), 478–482.

(3) Louis, D. N.; Perry, A.; Reifenberger, G.; von Deimling, A.; Figarella-Branger, D.; Cavenee, W. K.; Ohgaki, H.; Wiestler, O. D.; Kleihues, P.; Ellison, D. W. The 2016 World Health Organization Classification of Tumors of the Central Nervous System: A Summary. *Acta Neuropathol.* **2016**, *131* (6), 803–820.

(4) Rock, K.; McArdle, O.; Forde, P.; Dunne, M.; Fitzpatrick, D.; O'Neill, B.; Faul, C. A Clinical Review of Treatment Outcomes in Glioblastoma Multiforme--the Validation in a Non-Trial Population of the Results of a Randomised Phase III Clinical Trial: Has a More Radical Approach Improved Survival? *Br. J. Radiol.* **2012**, *85* (1017), e729-33.

(5) Stetka, B. New Strategies Take on the Worst Cancer--Glioblastoma. https://www.scientificamerican.com/article/new-strategies-take-on-the-worst-cancer-

glioblastoma (accessed Mar 1, 2022).

(6) The Brain Tumour Charity. Glioblastoma Prognosis - Brain Tumour Survival Rates. https://www.thebraintumourcharity.org/brain-tumour-diagnosis-treatment/types-of-brain-tumour-adult/glioblastoma/glioblastoma-prognosis/ (accessed Mar 1, 2022).

(7) American Association of Neurological Surgeons. Glioblastoma Multiforme - Symptoms, Dianosis, and Treatments. https://www.aans.org/en/Patients/Neurosurgical-Conditions-and-Treatments/Glioblastoma-Multiforme (accessed Mar 1, 2022).

(8) Siegel, R. L.; Miller, K. D.; Fuchs, H. E.; Jemal, A. Cancer Statistics, 2021. *CA. Cancer J. Clin.* **2021**, *71* (1), 7–33.

(9) Akins, N. S.; Nielson, T. C.; Le, H. V. Inhibition of Glycolysis and Glutaminolysis: An Emerging Drug Discovery Approach to Combat Cancer. *Curr. Top. Med. Chem.* **2018**, *18* (6), 494–504.

(10) Shen, Y.-A.; Chen, C.-L.; Huang, Y.-H.; Evans, E. E.; Cheng, C.-C.; Chuang, Y.-J.; Zhang, C.; Le, A. Inhibition of Glutaminolysis in Combination with Other Therapies to Improve Cancer Treatment. *Curr. Opin. Chem. Biol.* **2021**, *62*, 64–81.

(11) Hossain, M. I.; Thomas, A. G.; Mahdi, F.; Adam, A. T.; Akins, N. S.; Woodard, M. M.; Paris, J. J.; Slusher, B. S.; Le, H. V. An Efficient Synthetic Route to L-γ-Methyleneglutamine and Its Amide Derivatives, and Their Selective Anticancer Activity. *RSC Adv.* **2021**, *11* (13), 7115–7128.

(12) Qu, Y.; Han, B.; Yu, Y.; Yao, W.; Bose, S.; Karlan, B. Y.; Giuliano, A. E.; Cui, X. Evaluation of MCF10A as a Reliable Model for Normal Human Mammary Epithelial Cells. *PLoS One* **2015**, *10* (7), e0131285.

(13) Malavašič, Č.; Brulc, B.; Čebašek, P.; Dahmann, G.; Heine, N.; Bevk, D.; Grošelj, U.; Meden, A.; Stanovnik, B.; Svete, J. Combinatorial Solution-Phase Synthesis of (2 S ,4 S)-4-Acylamino-5-Oxopyrrolidine-2-Carboxamides. *J. Comb. Chem.* **2007**, *9* (2), 219–229.

(14) Bracci, A.; Manzoni, L.; Scolastico, C. Stereoselective Synthesis of a Functionalized 2-Oxo-1-Azabicyclo[5.3.0]Alkane as a Potential Scaffold for Targeted Chemotherapy Strategies. *Synthesis* **2003**, *15*, 2363–2367.

(15) Riofski, M. V.; John, J. P.; Zheng, M. M.; Kirshner, J.; Colby, D. A. Exploiting the Facile Release of Trifluoroacetate for the α-Methylenation of the Sterically Hindered Carbonyl Groups on (+)-Sclareolide and (−)-Eburnamonine. *J. Org. Chem.* **2011**, *76* (10), 3676–3683.

(16) Durand, X.; Hudhomme, P.; Khan, J. A.; Young, D. W. Two Independent Syntheses of (2S,4S)- and (2S,4R)-[5,5-2H2]-5,5′-Dihydroxyleucine. *Tetrahedron Lett.* **1995**, *36* (8), 1351–1354.

(17) Hossain, M. I.; Hanashima, S.; Nomura, T.; Lethu, S.; Tsuchikawa, H.; Murata, M.; Kusaka, H.; Kita, S.; Maenaka, K. Synthesis and Th1-Immunostimulatory Activity of α-Galactosylceramide Analogues Bearing a Halogen-Containing or Selenium-Containing Acyl Chain. *Bioorg. Med. Chem.* **2016**, *24* (16), 3687–3695.

(18) Bateman, L.; Breeden, S. W.; O'Leary, P. New Chiral Diamide Ligands: Synthesis and Application in Allylic Alkylation. *Tetrahedron: Asymmetry* **2008**, *19* (3), 391–396.

(19) Le Maux, P.; Nicolas, I.; Chevance, S.; Simonneaux, G. Chemical Reactivity of 6-Diazo-5-Oxo-l-Norleucine (DON) Catalyzed by Metalloporphyrins (Fe,Ru). *Tetrahedron* **2010**, *66* (25), 4462–4468.

(20) Moloney, M. G.; Panchal, T.; Pike, R. Trans-2,5-Disubstituted Pyrrolidines: Rapid Stereocontrolled Access from Sulfones. *Org. Biomol. Chem.* **2006**, *4* (21), 3894.

(21) Pichon, M.; Figadère, B.; Cavé, A. C-Clycosylation of Cyclic N-Acyliminium Ions with Trimethylsilyloxyfuran. *Tetrahedron*

Lett. **1996**, *37* (44), 7963–7966.

(22) Mitchell, R. E. Synthesis of Amino Acid Conjugates to 2-Imino-3-Methylene-5-Carboxypyrrolidine and 2-Imino-3-Methylene-6-Carboxypiperidine. *Bioorg. Med. Chem. Lett.* **2010**, *20* (6), 1910–1912.

(23) Hitchcock, P. B.; Rahman (née Masood), S.; Young, D. W. An Alternative to the Use of δ-Lactam Urethanes in the "Ring Switch" Approach to Higher Homologues of AMPA-Type Glutamate Antagonists. *Org. Biomol. Chem.* **2003**, *1* (15), 2682–2688.

(24) Hensley, C. T.; Wasti, A. T.; DeBerardinis, R. J. Glutamine and Cancer: Cell Biology, Physiology, and Clinical Opportunities. *J. Clin. Invest.* **2013**, *123* (9), 3678–3684.

(25) Shapiro, R. A.; Clark, V. M.; Curthoys, N. P. Inactivation of Rat Renal Phosphate-Dependent Glutaminase with 6-Diazo-5-Oxo-L-Norleucine. Evidence for Interaction at the Glutamine Binding Site. *J. Biol. Chem.* **1979**, *254* (8), 2835–2838.

(26) Wolf, M. A.; Claudio, P. P. Benzyl Isothiocyanate Inhibits HNSCC Cell Migration and Invasion, and Sensitizes HNSCC Cells to Cisplatin. *Nutr. Cancer* **2014**, *66* (2), 285–294.

(27) Yoo, G. H.; Piechocki, M. P.; Ensley, J. F.; Nguyen, T.; Oliver, J.; Meng, H.; Kewson, D.; Shibuya, T. Y.; Lonardo, F.; Tainsky, M. A. Docetaxel Induced Gene Expression Patterns in Head and Neck Squamous Cell Carcinoma Using CDNA Microarray and PowerBlot. *Clin. Cancer Res.* **2002**, *8* (12), 3910–3921.

Graphical Abstract